1. Introduction

1.1. Opening Remarks

The simple view of mass-wind balance in a tropical cyclone – that gradient balance applies everywhere except in the boundary layer – appears to be well supported by observations (La Seur and Hawkins 1963, Hawkins and Rubsam 1968, Willoughby 1990, 1991). While there are some dissenting voices (Gray, 1967, 1991) the differences seem to be an artifact of the analysis process.

The correspondingly simple view of the boundary layer is for a steady decrease in wind speed from gradient flow at the top at around 1 km, to a 10 m flow of around 0.7 times that, together with a progressive turning of the wind direction towards the storm centre. There is significant variation in the ratio of 10-metre to gradient-level wind speed, which will be discussed in detail later. The shape of the intervening profile has been less investigated, largely because observations of wind profiles in the tropical cyclone boundary layer were until very recently quite rare, due to the difficulty of taking measurements there. However, a considerable proportion of those early observations show the presence of low-level jets, variously reported as being at 60 m (Wilson, 1979), 200 m (Korolev et al., 1990), and 550 m (Moss and Merceret, 1976). In the recent past, the advent of the GPS dropsonde (Hock and Franklin, 1999) has yielded a wealth of new data on this phenomenon. For instance, Black and Shay (1998) in an initial report on recent observations from this instrument, state that “Nearly all high wind soundings show this feature [a low-level jet]”. High resolution modelling studies such as that of Li et al. (1997) also show a similar feature.

Such features are of practical importance. If the additional momentum was advected towards the surface by, say, a convective downdraft, it could have a

considerable impact on surface damage. It is thus important to operational forecasts and warnings, and should be considered in the design of high-rise structures. In areas where aircraft reconnaissance is available, it is necessary to estimate a near-surface wind from flight-level data, and various models have been used to "reduce" the flight-level winds to the surface (Powell 1980). Without exception, these models assume a monotonic profile. A similar application often occurs in storm surge modelling, where a suitable parametric gradient wind field and an estimated reduction factor are used to determine a surface wind field to force the ocean model (e.g. Hubbert et al., 1991). Clearly, departures from monotonicity and the large variation in observed reduction factors will impact the accuracy of these studies.

In this context it is interesting to note that the boundary-layer profile models don't perform any better than crude empirical techniques. When Powell (1980) tested a number of such models against aircraft and buoy data, he found that the empirical technique of simply multiplying the flight level wind by 0.8 was as good or better predictor of the near-surface wind speed than any of the physically based models. More recent work has tended to use either a profile model thus allowing the inclusion of stability effects (e.g. Powell 1982, Powell 1987, Powell et al. 1991, Powell et al. 1996) or the ratio approach (eg Frank 1984, Hubbert et al. 1991).

The lack of success of profile models, relative to the empirical ratio approach, is perhaps not surprising. For instance, the extrapolation of models conceived and tested in more benign environments into the severe conditions of the tropical cyclone core is not necessarily valid. Some of the assumptions of the profile models may be violated – such as the application of surface layer similarity theory up to the reconnaissance flight level of 500 m in the Cardone (1969) model. More generally, horizontal homogeneity

is a necessary assumption for such one-dimensional models, and this is likely to be violated in the strong gradients in the cyclone core, and at landfall. The application to aircraft data – typically taken between 500 m and 3 km – may exacerbate the problem since the adjustment time for the profile to re-attain equilibrium following changes in surface conditions or gradient-level wind will be longer for a deeper profile.

The possibility of supergradient winds in the boundary layer has received its most thorough theoretical treatment to date by Shapiro (1983), who used a slab model to calculate the depth-averaged boundary layer wind field for stationary and moving storms, and found a small area of boundary-layer supergradient flow just inside the gradient level radius of maximum winds in a stationary storm, and located towards the front and left of a moving storm in the Northern Hemisphere. Willoughby (1991) presented a relatively crude calculation with an assumed cross-contour flow angle in the boundary layer which also supported the possibility, while Mitsuta et al. (1988) presented observations of a slightly supergradient near-surface wind in Typhoon Vera of 1977. In each case, the winds were approximately 10% supergradient.

Explanations of the cause of these observed low-level wind maxima have also been sought by analogy with the well-known nocturnal jet (Blackadar 1957). There, nocturnal cooling produces such a strong stabilisation of the lower boundary layer that the flow above is effectively decoupled from the surface. The frictionally induced ageostrophic part of the flow then undergoes an inertial oscillation, until it is aligned with and adds to the geostrophic part of the flow, typically producing the strongest wind shortly before sunrise and at a height of a few hundred metres. Recent observations of air-sea temperature difference in cyclone cores, where the air is cooled to several degrees below the sea surface temperature (Korolev et al. 1990, Black et al. 1993, Cione

et al. 2000), have led to speculation that observed low-level jets arise from this mechanism. Clearly the analogy is not exact – the surface wind does not go to zero, and anemometer traces provide plentiful evidence of strong turbulence at the surface – so decoupling can not be complete. Moreover, the greater shear and lesser cooling in the cyclone leave the Richardson number much closer to zero than in the nocturnal boundary layer, with therefore a much larger vertical momentum transport. Another difference is that the nocturnal stable layer extends right to the surface, while the observations of Cione et al. (2000) suggest rather a shallow unstable layer immediately adjacent to the water surface, possibly with a stable layer above. However, it seems unlikely that stability could play a dominant role in the dynamics of the lower boundary layer in the core of a tropical cyclone, as the turbulence kinetic energy budget would be expected to be dominated by the shear production term there[1].

This thesis presents an analytical and a numerical model of the wind field in an idealised tropical cyclone boundary layer. The analysis will focus on two main features: (i) the physical mechanism which produces steady super-gradient flow in the upper part of the boundary layer, and (ii) the relationship between the near-surface winds and those aloft. The analytical model is presented and analysed in chapter 2, while the numerical

[1]Black and Holland (1995) presented evidence of strong stability and partial decoupling, with a diurnal modulation, on the western flank of Australian Tropical Cyclone Kerry of 1995. This was a special case for several reasons. Firstly, it was slow moving and so lay over a band of cold surface water to the south and west that had been produced by mixing and upwelling. Secondly, it was subject to significant westerly shear and so there was marked subsidence on the western side, which would have helped increase the stability there. Finally, the subsidence also suppressed the clouds and allowed a more marked diurnal variation in radiation than would normally be the case.

model is the subject of chapter 3. Following this is a comparison of the predictions from the two models with a range of observations. The final chapter contains further discussion and conclusions. The remainder of this chapter is devoted to a literature survey; firstly of observationally based studies of tropical cyclone boundary layer structure, followed by theoretical and modelling studies. It closes with a hypothesis of the mechanism responsible for the formation of the jet.

1.2 Observed Boundary Layer Wind Structure

Here, the state of knowledge of the observed tropical cyclone boundary-layer wind field is reviewed. We begin by reviewing the horizontal structure, followed by the relationship between near-surface winds and those aloft, then observed vertical wind profiles, and boundary-layer rolls. Although this classification is somewhat arbitrary, it is necessary to impose some order on the mass of material. While some of the studies cited focus specifically on the boundary layer, a substantial part of this review will rely on the lower atmospheric component of analyses prepared for other purposes.

The conventional observation network is inadequate for describing the low level structure of tropical cyclones. This is partly due to the general sparsity of observations in the tropics and particularly over the oceans, but also to the relatively small size of and sharp gradients within the core of a tropical cyclone. Moreover, instruments may not survive or be calibrated for the extreme conditions in the core, and ships actively avoid cyclones when possible, thus removing one important observation source. Thus most of the studies cited utilise special, nonroutine observing platforms, such as reconnaissance aircraft, especially deployed buoys and, more recently, airborne Doppler radar. Most analyses increase the data density by compositing, either over some period of an individual storm's life, during which it is assumed to be at a steady state, or by combining many storms. A particular problem with composite analyses of the boundary layer, which will be discussed further below, is that of combining observations taken at different heights in a region of strong vertical shear.

1.2.1 Horizontal wind structure

The majority of observational studies of tropical cyclones involve compositing of the data, either over some period of a storm's life, or over several storms. Indeed

composite studies date back to the very beginning of the study of tropical cyclones, since it was through the slow painstaking efforts in collecting data from eyewitness reports and ships logs through the early part of the nineteenth century that lead to the realisation that "This storm was exhibited in the form of a great whirlwind" (Redfield 1830). While this was a rediscovery of earlier work – Reid (1838) mentions Bacon and Capper in this context – further systematic and extensive collection of data by Redfield, Reid and Piddington (1848) enabled them to develop a picture of a giant whirlwind, in which a calm eye was surrounded by the strongest winds. They knew that in the Northern Hemisphere the most destructive winds lay in the right forward quadrant, relative to the direction of movement; that the pressure fell as the storm approached, reached a minimum in the eye, and rose again during the period of second winds; and that the surface flow consisted of an inwards spiral. Based on the "law of storms", of which this formed a part, mariners could recognise the early signs of an approaching tropical cyclone, and take action to stay out of harm's way, while those on shore could take precautions to reinforce or evacuate their buildings.

Perhaps the most comprehensive set of surface observations in a tropical cyclone over the open ocean was provided by the Japanese Imperial Navy in 1935, when a typhoon passed directly over the "Red" Fleet, during manoeuvres. Although the storm in question was undergoing extra-tropical transition with the associated structural changes, the analyses (Arakawa and Suda, 1953) confirm many of the features noted a century earlier by Redfield and his peers.

The need to warn for severe weather has always been one of the influences driving the establishment and improvement of meteorological services. As part of this, the United States established weather observing offices around the Carribean late in the

nineteenth century, largely to assist in the preparation of hurricane warnings. However, hurricane forecasts were often substantially limited by the lack of precise knowledge of the storm's location and intensity. Prior to the Second World War, the US Coast Guard had been briefly tasked with sending ships out specifically to take observations in hurricanes. However, due to the hazard and to the relatively low speed of movement of ships, nothing came of this. Improvements in aircraft technology and pilot training lead to a recognition of the possibilities that aircraft reconnaissance offered, which were fulfilled when USAF Lt Duckworth made the first (unauthorised) penetration in 1943. The effort increased rapidly, spurred on by the serious damage to the U.S. Third Fleet by two Pacific typhoons in 1944 (Tannehill, 1956).

It is appropriate to regard Hughes (1952) as the first composite study of the modern era, since he was the first to use the greatly increased observation density resulting from aircraft reconnaissance. Hughes took three years of North Pacific data from U.S. Navy flights, selecting 84 flights for which good central fixes were available. The data were positioned relative to the storm centre and motion direction, and analysed. Azimuthal and radial components, inflow angle, divergence and vorticity were also calculated. In contrast to the historical studies, Hughes found the strongest wind speed in the right rear quadrant, co-located with the strongest inflow. If the storm motion was subtracted from the wind vectors, the inflow maximum shifted to the right front. The maximum convergence formed an arc centred on the left rear quadrant, while there was weak divergence outside of about 200 km radius towards the right front.

Johnson (1954) presented an analysis of a single storm as it passed over Lake Okeechobee in Florida, using data from what would today be described as a surface meso-net. He did not present full wind analyses, but did show that the inflow angle was

a maximum in the rear of the storm, in agreement with Hughes (1952). Krueger (1959) presented analyses of storm-relative motion based on ship data for several hurricanes. He found two maxima in the inflow angle, in the right forward and right rear quadrants, with the smallest angles in the left rear (including weak outflow at larger radii there). He also showed that the asymmetric part of the storm-relative flow, which resulted in strongest winds in the left front and strongest inflow in the right front, could be approximately represented by a weak wind vector vector aligned from the right front to left rear.

The major composite study of Shea and Gray (1973) used 13 years of aircraft data from 533 radial flight legs undertaken by the National Hurricane Research Laboratory between 1957 and 1969. Of these, 61 were at altitudes between 500 and 1650 m and are thus relevant to the boundary-layer. The relatively small proportion at low altitudes highlights one problem with aircraft data for boundary studies – for safety reasons, observations are less common nearer to the surface. The observations were composited relative to the radius of maximum winds (RMW) and direction of storm movement, analysed, and assigned to a nominal altitude of 900 hPa. Their analyses of earth- and storm-relative azimuthal and radial winds are reproduced here as Fig 1.1. The azimuthal wind clearly shows a maximum slightly forward of the right-hand side of the storm. This is weaker but still present when the storm motion is subtracted. The azimuthal-mean radial flow has strong inflow decreasing towards the RMW, and weak outflow inside. This flow is however strongly asymmetrical, with marked through-flow from right-rear to left-front of the storm in earth-relative coordinates. When the storm motion is subtracted, the inflow maximum shifts to the right-forward quadrant, with marked outflow on the left-hand side at about the RMW. The asymmetries are clearly related to the motion. Unfortunately Shea and Gray did not attempt to further stratify

the data by speed of motion, probably due to a shortage of data. The mean speed of the movement was not given, although comparing their earth and storm relative plots indicates it is between 3 and 5 m s^{-1}.

Frank (1977a) conducted a similar composite study of North West Pacific Typhoons, using 10 years of rawinsonde and surface data. He tended to have better coverage of the outer part of the storm than Shea and Gray (1973), but less data in the eye. The azimuthal mean azimuthal flow shows a maximum at a height of about 850 hPa in the core, sloping gradually down to 900 hPa at 1000 km radius, while the azimuthal mean radial flow showed that the inflow became stronger and slightly shallower towards the core. His analyses of the asymmetric flow were presented in an earth-oriented coordinate system, to better depict the upper tropospheric outflow. This coordinate system is not optimal for depicting the boundary layer, where the asymmetries tend to be oriented with the storm motion. However, analyses in motion-oriented coordinates were presented in Frank (1976). These show the 950 hPa inflow is a maximum slightly forward of the right of the storm in the earth-relative motion-oriented coordinate system. Relative to the storm, the strongest boundary layer inflow was directly in front, and was about twice as strong to the right of the storm as to the left.

Some of the aircraft data used by Shea and Gray (1973) were also used in two case studies of individual storms. An analysis of the nominal 900 hPa cyclone-relative wind speed in Hurricane Hilda of 1964 (Hawkins and Rubsam, 1968) shows a similar asymmetry to that of Shay and Gray (1973), along with some outer maxima associated with rain bands (Fig 1.2). They did not present an analysis of the full radial flow, arguing that small errors in aircraft navigation can lead to substantial errors in the calculated

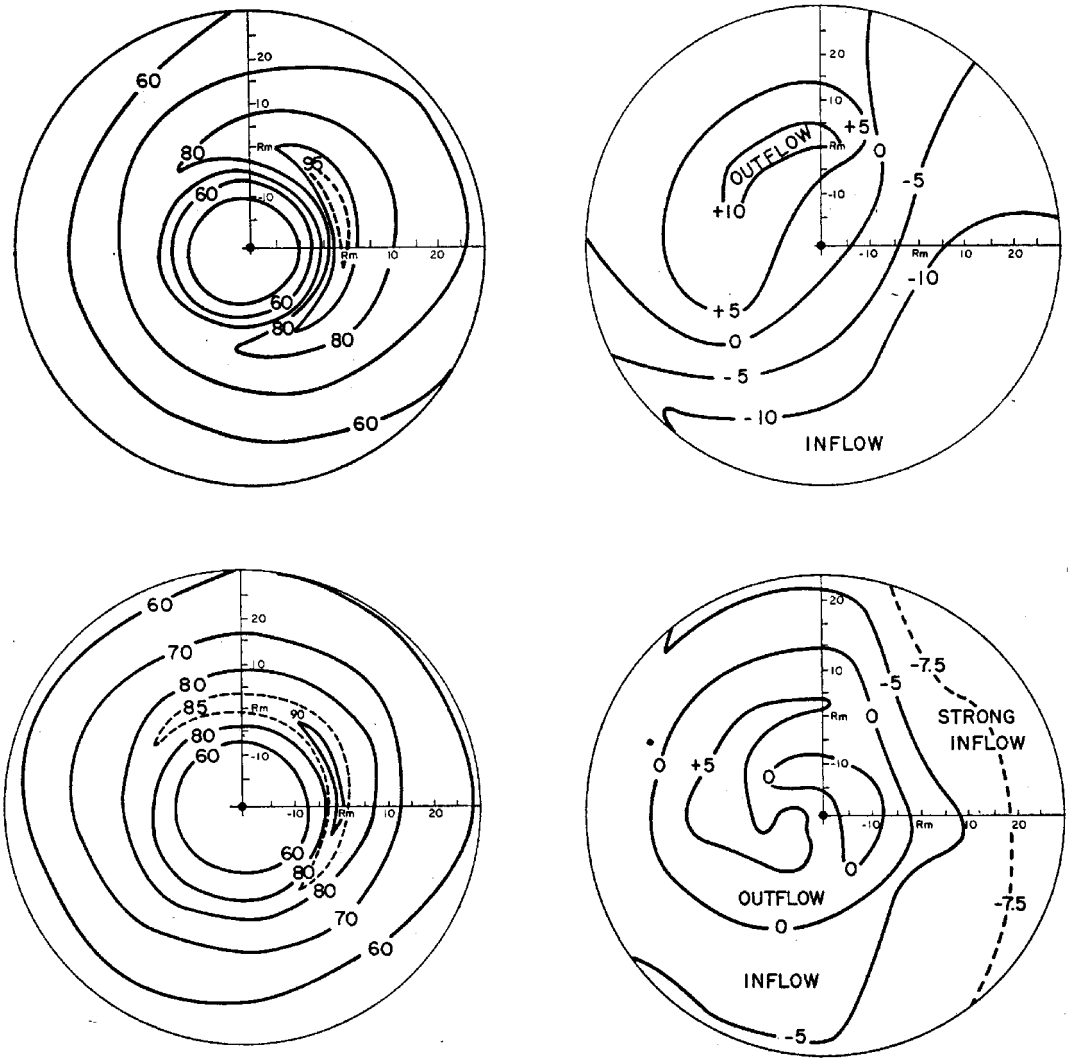

Figure 1.1 Composite wind field at 900 hPa (nominal). Azimuthal wind (left) and radial wind (right) in earth-relative (top) and storm-relative (bottom) coordinate systems. Storm movement is towards the top of the page. From Shea and Gray (1973).

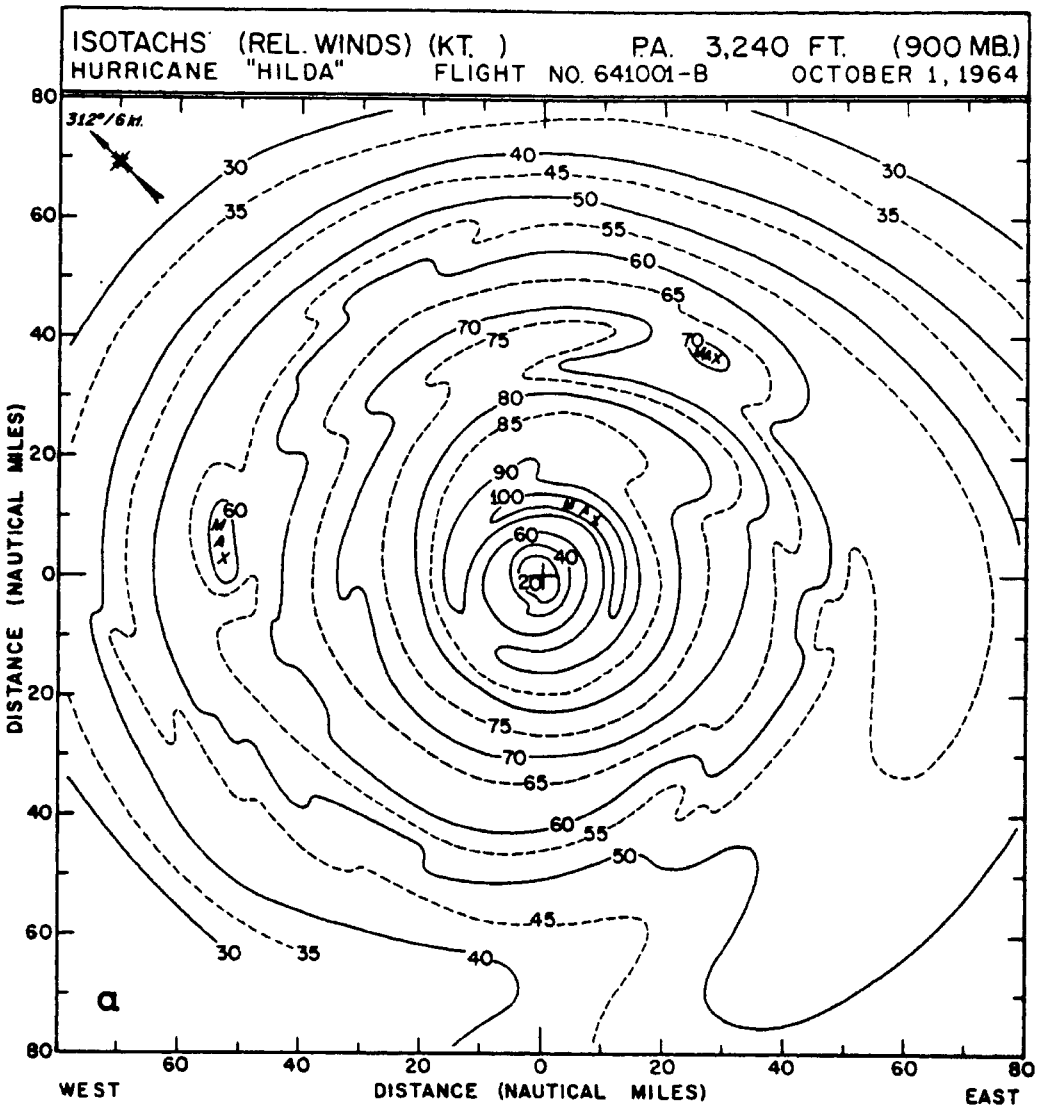

Figure 1.2 Isotachs at 900 hPa in Hurricane Hilda. The arrow in the top left shows the storm movement. From Hawkins and Rubsam (1968).

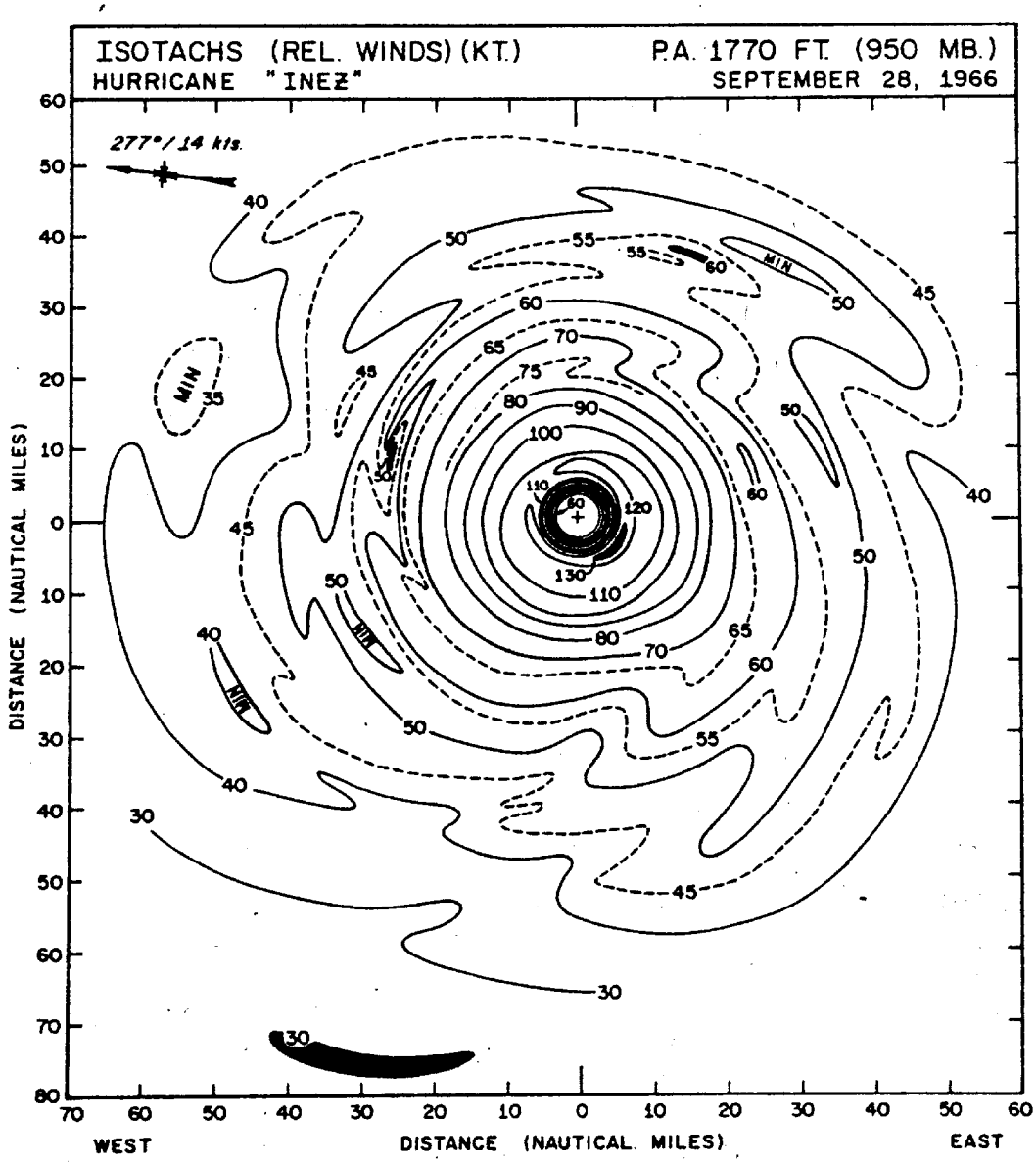

Figure 1.3 Same as for Fig 1.2, but at 950 hPa in Hurricane Inez (right). Note that the domain sizes is smaller in this case: 130 n.m rather than160 n.m. From Hawkins and Imbembo (1976).

radial flow, but did give an azimuthally averaged estimate, constrained by mass continuity, which shows a tendency to a shallower and stronger inflow layer towards the core. A similar analysis for Hurricane Inez of 1966 (Hawkins and Imbembo, 1976) presents a contrasting picture, with the speed maximum at 900 hPa in the left rear quadrant (Fig 1.3). This appears to be due to an overall storm asymmetry, rather than storm motion, as the maximum is in a similar location at the other two levels analysed, 700 and 180 hPa (not shown here). Inez was noted to be a comparatively small storm, with a correspondingly peaked radial wind profile. Azimuthally averaged inflow was estimated, and comparison of the relevant figures shows the inflow in Inez was two to three times as strong as in Hilda, at the same radius.

Hurricane Frederic of 1979 has been the subject of two important studies. Powell (1982) composited buoy, ship, aircraft and land-based observations over two periods to produce analyses of the surface wind field over the ocean and at landfall. Data were adjusted to a common height of 10 m by a one-dimensional boundary layer model. For surface-based observations, this required a small change, but larger reductions were applied to aircraft observations. Corrections for different wind-averaging periods between the various observational platforms were argued to be unnecessary. His analysed surface flow for the open-ocean case is reproduced in Fig 1.4. The maximum (earth-relative) wind speed is in the right forward quadrant. Inflow angles are largest to the right rear, and close to zero or negative on the left-hand side of the storm. A secondary maximum outside the RMW was associated with a spiral rainband (Jorgensen, 1984a). Powell's landfall composite shows increased inflow angle over land due to the greater friction, and the development of a secondary wind maximum in the offshore flow to the left of the storm (not shown here).

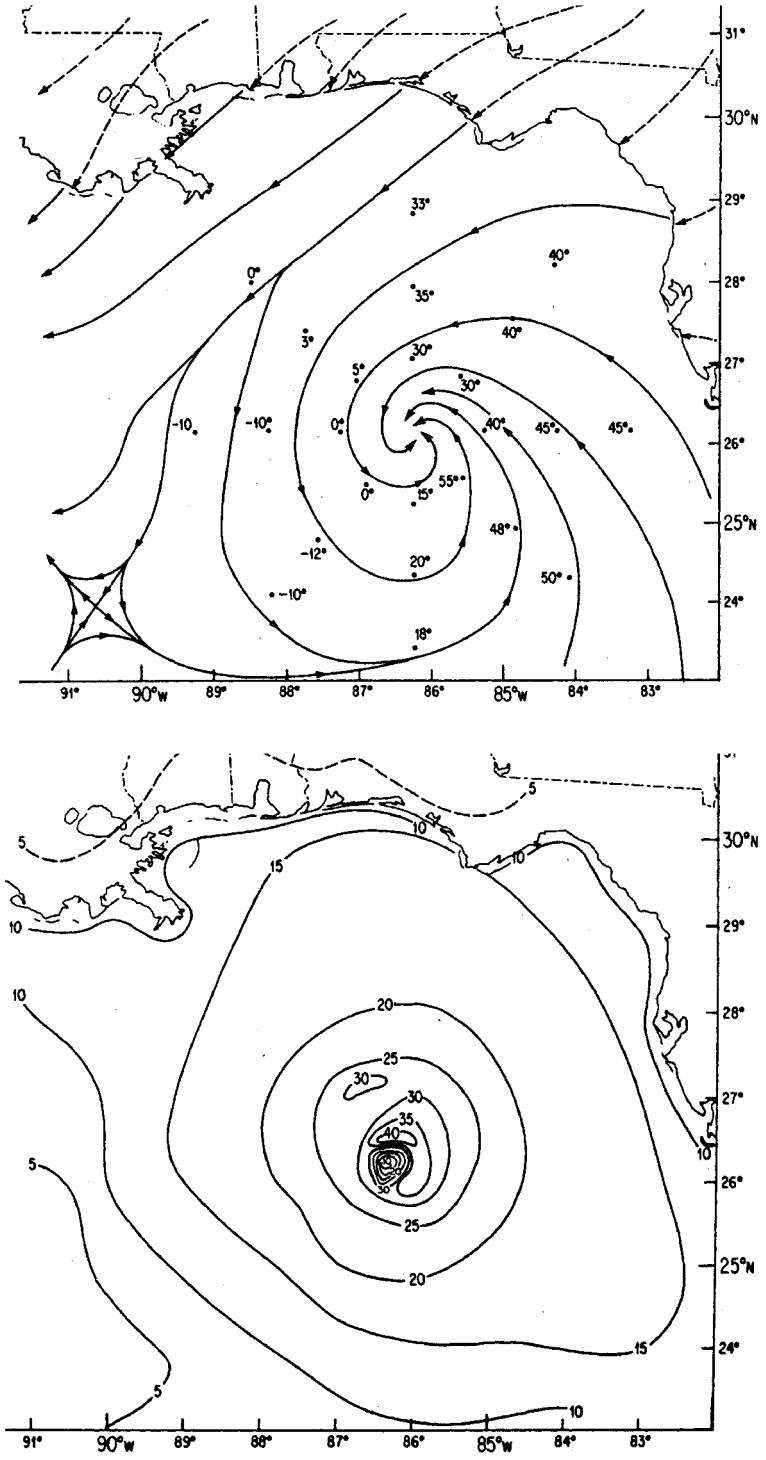

Figure 1.4 Near-surface streamlines and inflow angles (top) and isotachs (bottom) for Hurricane Frederic over-water composite at 1600 UTC on 12 Sept, 1979. From Powell (1982).

The same data were analysed at three levels, (surface, 560 and 1600 m), by Frank (1984). Aircraft data appear to have been used twice, both at the level of observation and reduced to the surface by multiplication by 0.7, or 0.6 if the observed inflow angle exceeded 20°. The azimuthally averaged tangential wind showed little shear above 560 m, being generally less than 5 m s^{-1} stronger at 1600 m. The updraft was about twice as strong at the upper level, peaking at 0.3 m s^{-1}, while a radius-height section of the azimuthal mean radial flow (Fig 1.5) showed strongest inflow at the surface, but a weak outflow within the eye. The contour of zero radial flow sloped downwards from above 2 km at a radius of 150 km, to near the surface in the eye, and its height was shown to scale approximately as $(f + V/r)^{-1/2}$ outside the RMW, where f is the Coriolis parameter, V the gradient wind speed and r the radius. The asymmetry in the storm-relative radial flow (Fig 1.6) consisted of through-flow from the right-front to left-rear, similar to that found by Shea and Gray (1973). The magnitude of the right forward quadrant inflow decreases, while that of the left rear quadrant outflow increases with height; thus it appears that the magnitude of the asymmetric radial component decays less rapidly with height than does the azimuthally averaged inflow. It is clear from Fig 1.6 that this asymmetry also rotates slowly anticyclonically with height. Frank found a maximum in the surface convergence field to the right of the storm. This is still evident at 560 m, where it was accompanied by marked divergence at the centre which also extended weakly out towards the left rear. Frank also calculated the surface drag coefficient from the residual term in the azimuthally averaged angular momentum budget. In contrast to the earlier similar calculations of Hawkins and Rubsam (1968) and Hawkins and Imbembo (1976), Frank found no increase of C_D with wind speed. This was shown to be primarily due to the use of an inflow layer depth which decreased markedly towards the centre in the budget calculation, rather than the constant value used in the earlier studies.

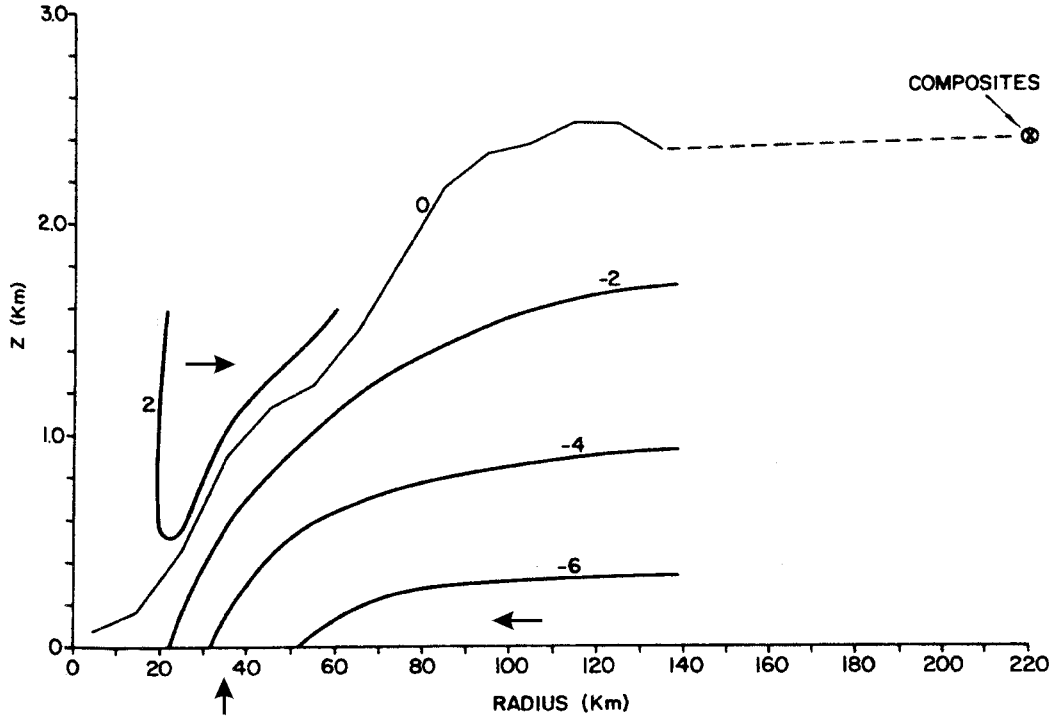

Figure 1.5 Vertical cross-section of the azimuthal mean radial wind in Hurricane Frederic. Note the decrease in height of the inflow layer towards the centre. The depth of the inflow layer at 2° radius in Frank's (1977) composite is also shown, and the arrow on the radius axis indicates the RMW and the radius of maximum azimuthal mean updraft at 560 m. From Frank (1984).

Hurricane Allen of 1980 received an unprecedented level of aircraft coverage, including multiple coordinated passes at five levels by three aircraft on a single radial track extending through the front right quadrant and the strongest winds (Jorgensen 1984b). Whilst most of the data were collected between approximately 1.5 km and 6 km, two passes were flown at 450 m, data from one of which was presented. During the first observational period on August 5th, the maximum tangential winds were about 70 m s^{-1} at a radius of 35 km and height of 1 km, while the peak inflow observed at the 450 m flight level was in excess of 25 m s^{-1}, at about 50 km radius. At this time, the radial component at 1.5 km was close to zero outside the RMW, demonstrating the shallowness of the frictional inflow layer, although the near-surface inflow layer did deepen through the day. The inflow at the lowest flight level extended inwards through the RMW to a radius of approximately 15 km. Above it lay a band of outflow, which strengthened as it sloped up the inside of the RMW. The maximum updraft was located a few km inside of the RMW, while the maximum radar reflectivity lay outside it, due to the rain falling through the outwardly sloping RMW. The analyses also show marked variation from one pass to the next, which was attributed to the passage of convective-scale features and some remnant eyewall cloud (from a previous eyewall contraction cycle) near the centre. While these results are highly interesting, Allen was within 200 km of Jamaica during this period and it is unclear to what extent the proximity of land affected the results. Further flights three days later, when the RMW had contracted to about 15 km and the central pressure fallen to 920 hPa, were at levels too high to reveal the boundary layer structure.

Powell (1987) applied similar techniques from his earlier Frederic study to Hurricane Alicia of 1983. Here, the over-ocean wind speed maximum lay at the front of the storm, with secondary maxima at two to three times the RMW on either side of the

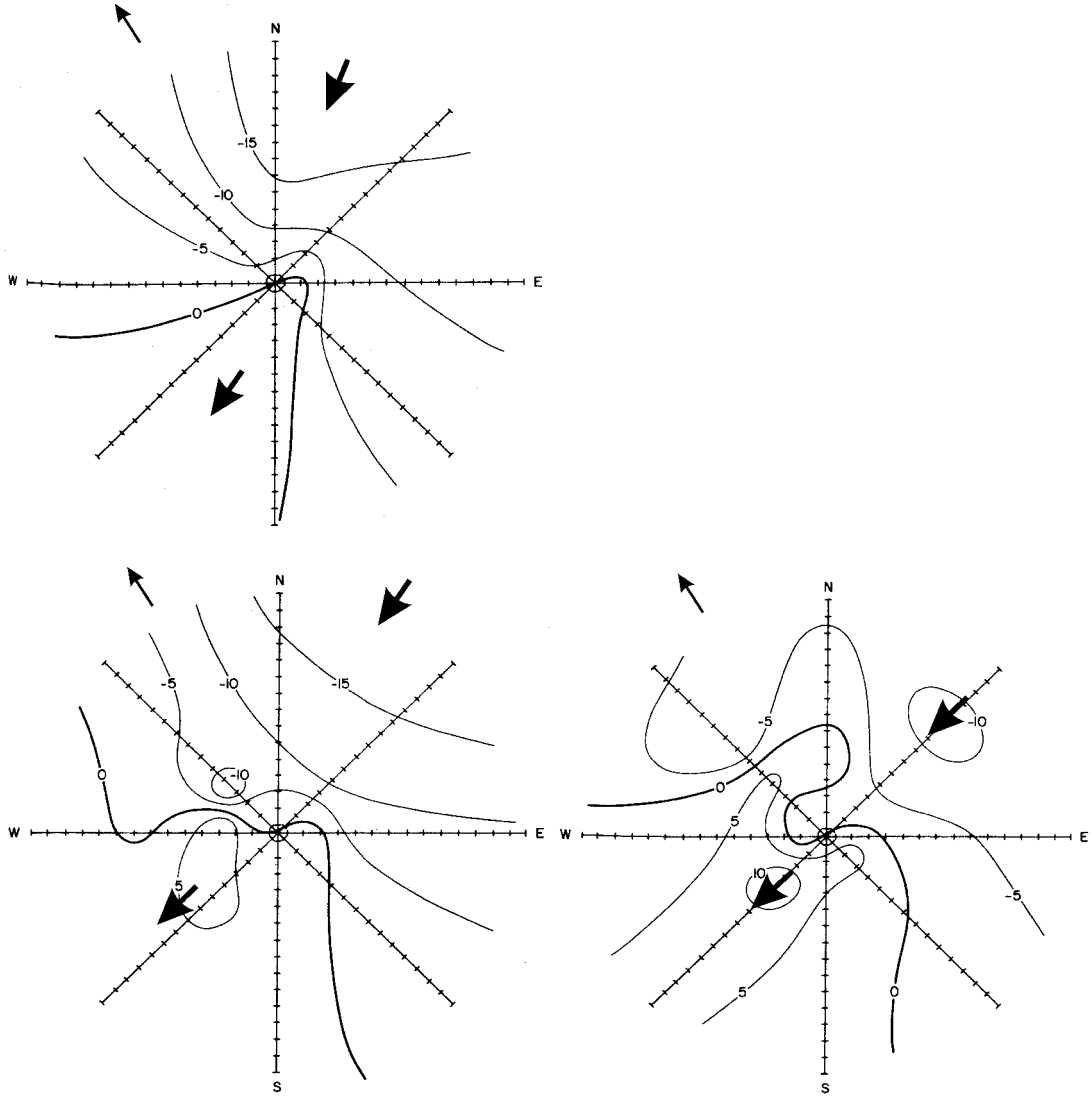

Figure 1.6 Isotaches of storm-relative radial wind at the surface (top), 560 m (lower left) and 1600 m lower (right). The light arrows show the storm movement, while the heavy arrows mark the areas of maximum relative inflow and outflow. From Frank (1984).

storm, associated with rainbands. At landfall, there was a single maximum to the right of the storm, while the radial flow showed strong right to left through-flow. A further study, of Hurricane Hugo (Powell et al. 1991) included the calculation of the observed surface to aircraft wind speed ratio as the storm made landfall (their table 1). Two stations with marine exposure are particularly interesting; one to the right of the storm reported ratios between 0.58 and 0.70, consistent with their one-dimensional profile model if stable stratification is assumed. The other, on the left of the storm, showed very high ratios of 0.99 and 1.21, which Powell suggested may have been due to strong static instability and a wind speed maximum below flight level. Wind profiles derived from aircraft Doppler radar showed some evidence of such a maximum near 1.5 km altitude.

Hurricane Andrew received a similar analysis (Powell et al. 1996, Powell and Houston 1996), with further advances in adjusting wind observations to a common framework. The main features of the analysed surface wind field were similar to the earlier cases. Surface wind factors calculated from observations were also tabulated. While there is a mix of marine and land exposure in the tables, two points to note are that the mean factor was 0.72 for observations within 34 km of the centre, and 0.63 outside, and that two anomalously high values, of 0.97 and 1.03, were calculated from observations taken on the yacht *Mara Cu*, close to the RMW on the left hand side.

The procedures used by Powell and his coworkers in preparing these analyses have been largely automated (Powell et al. 1998) and this has lead to a substantial increase in the number of analyses available – for instance, Powell and Houston (1998) consider 5 storms from the active 1995 season. These confirm the overall thrust of the earlier studies in that the wind maximum is generally found to the right of the storm, but that there is room for variation between storms or in the same storm at different times.

Similar analyses are now routinely prepared operationally for the U.S. National Hurricane Centre.

The study by Black et al. (1988) of Hurricane Josephine is important because of the unusually large amount of buoy data available. This was due to the special deployment by air of three meteorological and oceanographic buoys ahead of the storm, in its predicted path, which allowed the comparison of aircraft-derived to buoy-measured surface pressure and wind through the centre of the storm. Excellent agreement was obtained for pressure, while the surface winds (shown in Fig 1.7), reduced from the aircraft observations by Powell's (1980) column model[2], were also in good agreement except at the front eyewall where there appeared to be some marked tilt of the RMW with height. They produced two analyses of surface wind speed, one based upon aircraft data only, and the other upon buoy data, reproduced here in Fig 1.8. Both show the same broad structure, although the secondary maxima to the left of the track are better resolved by the buoy analysis. The aircraft analysis also has a narrower wind maximum, and its 40 m s^{-1} contour misses the buoy winds of that strength at the front of the storm, while the 35 m s^{-1} contour extends further around to the rear. In short, the analysis using aircraft data reduced to the surface has a narrower maximum, located further to the rear, than the analysis using buoy data.

Black and Holland (1995) presented composite analyses of the Southern Hemisphere Tropical Cyclone Kerry on two consecutive days, using ship, island and three levels of reconnaissance aircraft observations (500 m, 5.5 km and 7 km). Kerry was an asymmetric storm in a strongly sheared environment, and performed a slow loop during the study period. On both days, the azimuthal flow showed little shear to the

[2]This model is discussed in detail in section 1.3.4.

northeast of the storm, but was close to twice as strong at the lower level compared to the upper levels, to the southwest. This was to the left of, and behind, the storm motion on the two days. The low-level radial flow was inwards to the east to the east of the storm, and outwards to the west, on both days, with the direction of the radial flow at the upper levels tending to be the reverse of this due to the strong environmental shear. Analyses of the surface flow show a double maximum within the RMW, with maxima to the northeast and southwest of the centre on both days. The southwest maximum lay over an area of cold surface water, produced by upwelling and mixing, and they argued that the reduced stability there contributed to the maximum through partial frictional decoupling. Wind flight observations from Willis Island, some 400 km to the west of TC Kerry, show a maximum around 1 km in altitude with a marked diurnal variation. Three aircraft soundings were taken between 130 km and 260 km to the west of the storm, two of which show a marked wind speed maximum at around 900 hPa, while the other has fairly constant speed above 900 hPa, but marked shear below.

Several of the above studies have shown outer wind maxima, often in association with a spiral rainband. Such secondary wind maxima were investigated systematically using aircraft data by Samsury and Zipser (1995). Secondary maxima were found in over 20% of radial legs, and frequently lay within 20 km of radar reflectivity maxima. However the converse relationship did not hold, and over 70% of the rainbands found were not associated with wind maxima. The kinematic structure across a maximum was shown to be similar to that at the eyewall, with strong convergence due to flow into both sides of the maximum in the lower troposphere, but mostly from the inside at mid-troposphere. The mid-troposphere inflow was quite weak, confirming that the bulk of the radial mass flow occurred below 1 km. The preferred updraft location was just inside the horizontal wind maximum, for both primary and secondary maxima. Their use of a

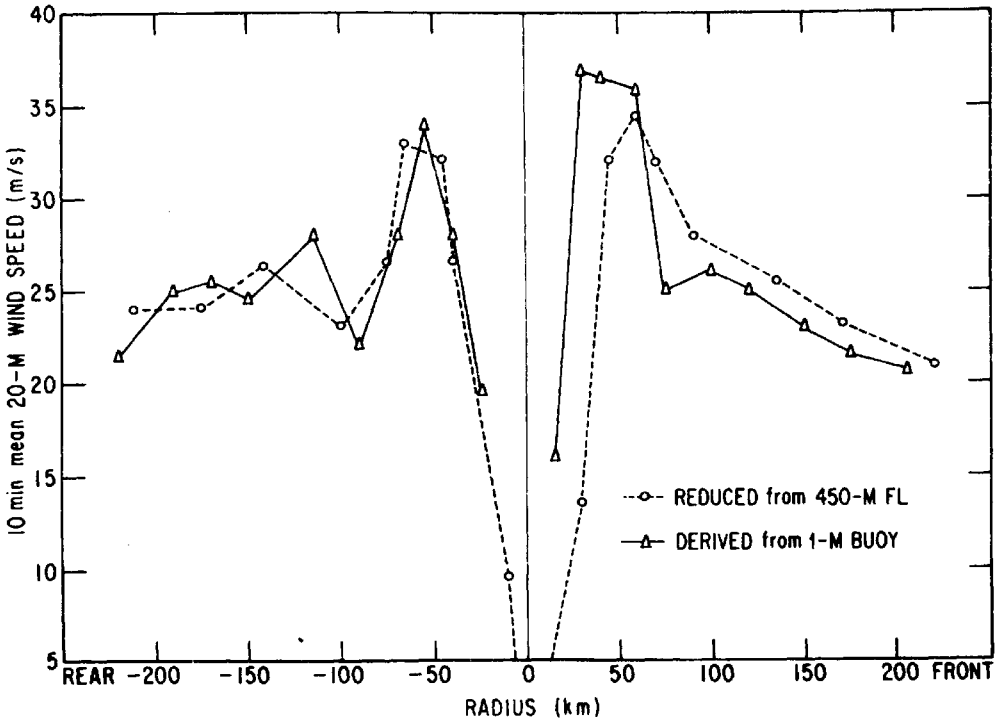

Figure 1.7 Comparison of buoy-measured near-surface winds with aircraft winds reduced to 10 m using a boundary-layer model, in Hurricane Josephine. From Black et al. (1988).

large data set thus systematised and confirmed the results from a number of case studies of the kinematic structure near hurricane rain bands, such as Powell (1990a, 1990b), and Barnes and Powell (1995).

Information about the near-surface winds may be derived from observations of the sea state. This can range from subjective techniques such as described by Black et al. (1986), who present some fascinating photographs of the progressive change in the appearance of the sea as the wind speed increases, to the more objective methods, such as the use of scatterometers. The latter measure the radar cross-section of the sea surface due to Bragg scattering from capillary waves, and may be mounted either on aircraft or satellites. Although scatterometers have been in existence for roughly three decades, there is little in the literature on their application to tropical cyclones. Two studies (Hsu and Liu 1996, Jones et al. 1999) demonstrate their clear utility in locating the centre, although intensity estimation is limited by factors including rain attenuation and backscatter of the radar beam, lack of resolution of the tight horizontal gradients, and uncertainties in calibration at extreme wind speeds. However these early studies shed little light on the structure. Known limitations include verification of the calibration at high wind speeds, the effect of horizontal averaging, the removal of ambiguous wind solutions, and the multiple effects of rain on the backscattered signal including attenuation, direct backscatter from rain, and changes to the sea surface roughness. Thus care will be needed if these data are to be used to improve our understanding of the surface wind structure under the high wind conditions in a tropical cyclone. However, the high frequency and large domain of coverage, particularly with the more recent broad-swathe instruments, suggests that there may be a wealth of information to be gleaned in future studies.

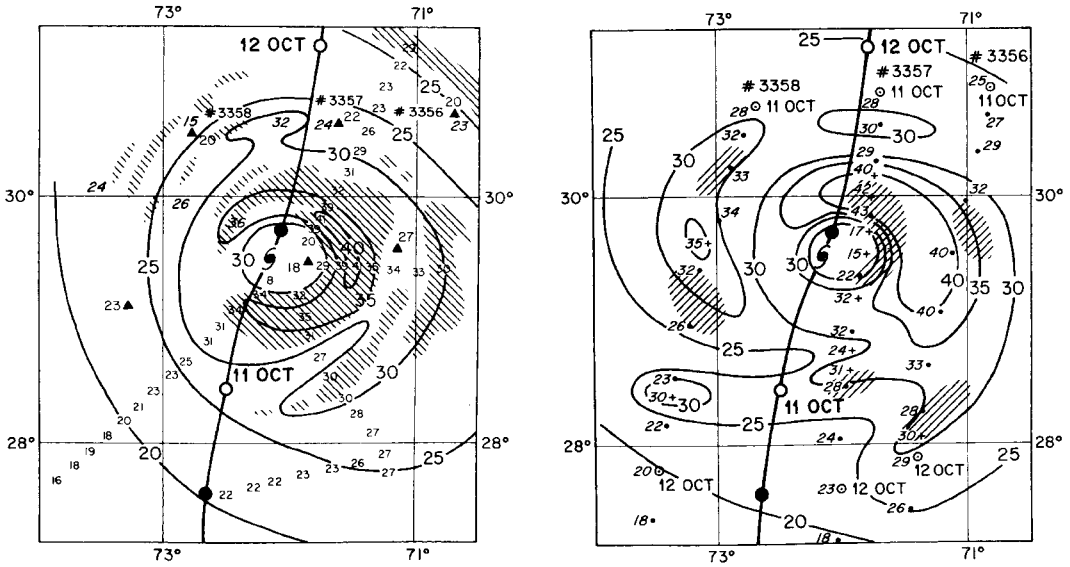

Figure 1.8 Surface isotach analyses in Hurricane Josephine based on aircraft data reduced to 10 m (left) and buoy data (right). On both panels, the heavy solid line shows the storm track with 1200 UTC (solid circles), 0000 UTC (open circles), and 1100 UTC on Oct 11 (hurricane symbol) superimposed. Cross-hatching on the left panel shows area where the radar reflectivity exceeded 25 dBz. On the left panel, the small numbers are the 20 m wind calculated from the research aircraft observations, and the solid triangles with adjacent numbers show the storm-relative buoy observations at the time of the aircraft flights. The slanted numbers are winds calculated from Air Force observed winds. On the right panel, the small numbers are the buoy observations of wind speed, plotted relative to the moving storm. The open circles indicate the 0000 UTC buoy positions relative to the storm, dots indicate 3-hr positions, and crosses important intermediate positions. From Black et al. (1988).

1.2.2 Observational Comparisons of Boundary Layer and Surface Winds

Clearly, a common theme in the surface wind analyses listed above is that almost all have relied upon aircraft observations, processed in some way to give an estimate of the surface wind. These range from the use of one-dimensional boundary layer models in the studies by Powell and his coworkers discussed above, to simply multiplying the aircraft wind speed by some "surface wind reduction factor", as done by Frank (1984). These techniques are useful not just for research purposes, but they also play a vital role in the preparation of forecasts and warnings using aircraft reconnaissance data. Powell (1980) evaluated four physically based column models and two empirical techniques, by applying the techniques to nineteen aircraft observations at approximately 500 m, for which there were nearly colocated surface observations. He found that three of the column models, as well as the empirical technique of simply multiplying the aircraft wind speed by 0.8, produced speed errors of around 10%, and were therefore satisfactory, while the remaining two techniques substantially underestimated the surface wind. Wind direction errors were not assessed. Of these models, the one that has since been frequently used is reviewed in Section 1.3.4.

Powell and Black (1990) presented a largely observational study of the ratio of surface to gradient wind speed. They found that values generally ranged from 0.55 to 0.85, although there were a significant number of outliers on either side of this range. Their scatter plot of the ratio as a function of buoy-measured air-sea temperature difference is reproduced here as Fig 1.9 and shows a clear stability dependence, as well as the degree of scatter. A table of mean ratios and their standard deviation as a function of air-sea temperature difference and flight level is reproduced in part here as Table 1.1. The following points are clear:

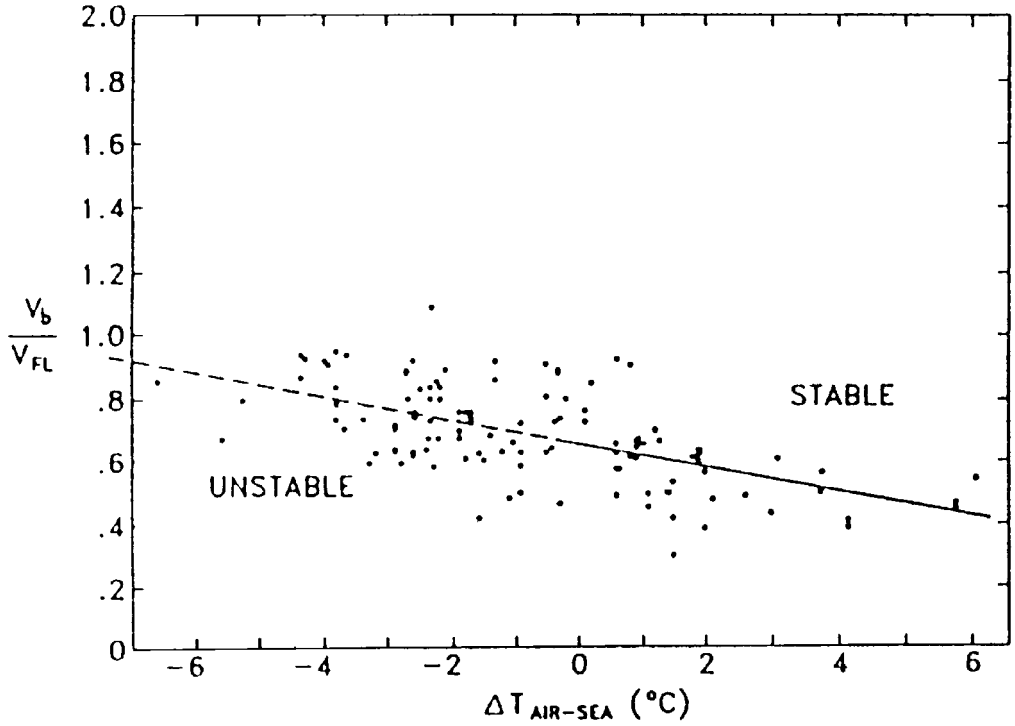

Figure 1.9 Scatter plot for the ratio of the measured surface wind speed V_b to the flight-level wind speed V_{FL} as a function of air-sea temperature difference. From Powell and Black (1990).

- The mean ratio decreases with increasing stability, and from the data in the table, there is less difference between neutral and unstable cases, than between neutral and stable.
- The mean ratio is smaller for flight-level data between 1001 and 2250 m than for data either above or below this, which can be regarded as being due to the wind speed maximum often observed at this level and discussed in more detail below.
- The standard deviation of the ratio is (unsurprisingly) smallest for flight-level data near the surface, but is largest for data in the intermediate range. That is, it appears that this technique will give less reliable estimates of surface wind speed when applied to aircraft observations taken at around 1500 m, than to observations from higher (or lower) levels. It is also smaller for stable, than unstable, situations.

Dobos et al. (1995) compared land-based surface measurements of wind speed and gustiness to boundary-layer profiler wind observations between 600 and 1800 m above the surface. They found that the mean ratio was somewhat lower than that of Powell and Black (1990), which they attributed to increased surface roughness over land. They also found a significant diurnal variation in the wind speed ratio, due to stability effects. This was most marked at low to moderate wind speeds, but was absent above 30 m s^{-1}.

The observed surface wind speed was compared to the calculated gradient wind in two typhoons, using observations from flat coral islands to the south of Japan, by Mitsuta et al. (1988). They found that while the ratio of surface to gradient wind speed was nearly constant outside the RMW, it increased rapidly inside and could exceed 1 on the inner side of the eyewall; that is, the wind speed at 10 m was supergradient. Results

Flight level	$T_s - T_a$ (°C)	No of comparisons	Mean ratio	Std dev
0 – 1000 m	< −1	9	0.55	0.08
	−1 to 1	16	0.71	0.1
	> 1	38	0.74	0.1
	All	63	0.7	0.12
1001 – 2250 m	< −1	14	0.47	0.09
	−1 to 1	6	0.71	0.18
	> 1	16	0.71	0.18
	All	36	0.61	0.19
2251 – 4000 m	< −1	5	0.65	0.08
	−1 to 1	8	0.63	0.11
	> 1	15	0.73	0.19
	All	28	0.69	0.16
All heights	< −1	28	0.51	0.1
	−1 to 1	30	0.69	0.12
	> 1	69	0.73	0.14
	All	127	0.67	0.16

Table 1.1 Mean and standard deviation of the surface to flight level wind speed ratio, as a function of flight-level and air-sea temperature difference. From Powell and Black (1990).

from one of their cases, Typhoon Vera, is reproduced here as Fig 1.10. Note the rapidly increasing ratio of surface to gradient speed on the inner side of the eyewall, where the surface inflow decreases towards zero. They suggest this was due to strong inflow and advection of angular momentum, and relate it to the outward flow in the upper part of the boundary layer inside the RMW observed by Shea and Gray (1973). Gray and Shea (1973) had also argued for supergradient winds just inside the RMW throughout the lower troposphere, but Willoughby (1990) was unable to reproduce their results and cast sufficient doubt on their analysis technique that it seems preferable not to give their results much credence here. Willoughby's (1990) comparisons show that the flow is very close to being in gradient balance, but his observations are generally above the boundary layer, with the case closest to the surface (900 hPa) being a very weak storm.

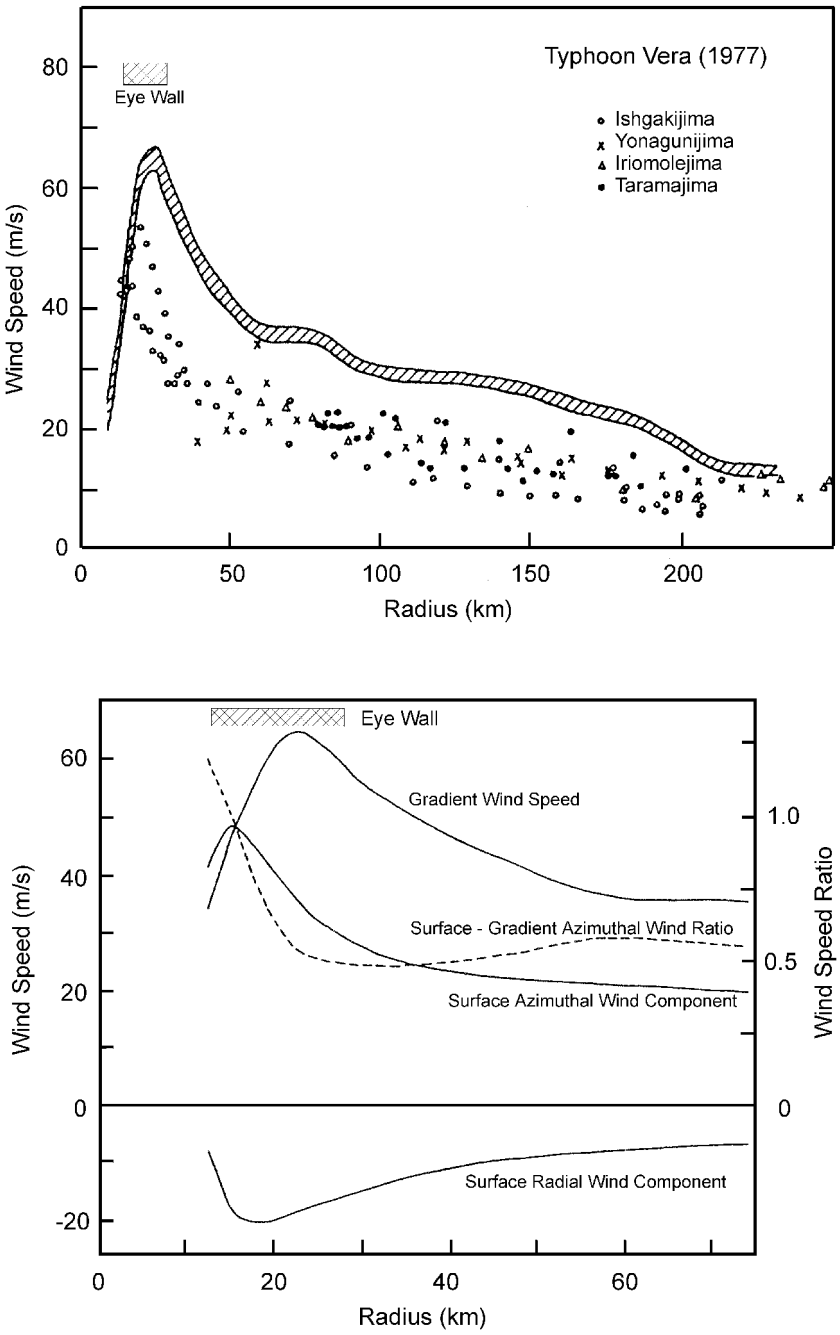

Figure 1.10 Surface winds in Typhoon Vera of 1977. Top: Observed surface wind speed (points) and calculated gradient wind speed range (shaded band) as a function of distance from the storm centre. Bottom: Radial and azimuthal components of the surface wind, the gradient wind speed, and the ratio of surface azimuthal to gradient speed in the typhoon core. Adapted from Mitsuta et al. (1988).

1.2.3 Observed Vertical Profiles of Boundary-Layer Wind

Aircraft soundings of wind, temperature and humidity, taken in a cloud-free area in the periphery of the weak Hurricane Eloise were presented by Moss and Merceret (1976). They found a double wind-speed maximum, with weak maxima of 22 m s^{-1} at 150 m and 550 m, and a 20 m s^{-1} minimum in between. The potential temperature profile was nearly constant to 650 m with a marked inversion above, so the wind maxima appears to both lie within the boundary layer. The moisture sounding was consistent with this interpretation of boundary-layer depth, showing its largest gradient above 650 m. Fast-response measurements were also taken, and analysis of the turbulence kinetic energy (TKE) budget equation between 400 and 650 m by Moss (1978) showed that the buoyant production was much larger in the upper boundary layer than the shear production, and had a maximum at about 500 m. This was balanced by transport away from the production maximum, and by dissipation. However, the residual term, which includes the time tendency of TKE, lateral shear production, horizontal advection and pressure-work contributions, was of similar magnitude to the resolved terms. Since it appears (assuming stationarity and valid measurements) that a large energy source term was not determined, it is difficult to know how much weight to give these results.

An alternative to aircraft sounding for obtaining wind profiles in the tropical cyclone boundary layer is the use of Doppler radar. Powell and Black (1984) presented wind profiles derived from an airborne Doppler radar, as well as stepped descents, along a rainband in Hurricane Debby. Profiles at the outer end of the band showed a maximum in the along-band component generally below 1 km; this became more marked and increased in height to be generally between 1 and 1.5 km towards the storm centre. Powell (1990a,b) further studied the mesoscale structure near rainbands with this technique in Hurricanes Josephine and Earl and found marked variation in structure, both

along and across the band. There was generally a wind speed maximum on the outer side of the rainband at about 1.5 km, with weaker flow on the inside. There was also some evidence of a speed maximum below 600 m, associated with the strong inflow component. Horizontal convergence and upward motion were a maximum on the inner side of the band, where there was a rapid decrease of inward cross-band flow component. Stepped-descent profiles in Hurricane Earl showed weak wind-speed maxima around 400 m on the inner side of the rainband.

Korolev et al. (1990) presented a profile of wind speed obtained from a ship-launched balloon in Typhoon Tess, which showed a wind speed maximum near 200 m. They also presented observations of air-sea temperature difference taken in Typhoons Tess and Skip, which showed that the air became up to 6 degrees cooler than the sea as the wind speed approached 25 m s^{-1}. The temperature profile obtained showed a distinct inversion from the surface to 100 m, and they speculated that this was evidence of sea spray evaporation. Cione et al. (2000) analysed buoy data from 37 hurricanes and found a similar, though weaker, signal which they showed was mostly due to a marked reduction in the air temperature between 125 and 325 km from the storm centre. As the pressure drop over this range was small, they concluded the temperature drop was not due to adiabatic expansion. Based also on their analysis of a smaller amount of humidity data, which showed the cooling was accompanied by a drying of the inflowing air, they suggested that the cooling was due to convective downdrafts. Barnes and Bognor (2001) analysed dropsonde data and found a similar cooling near the surface, which they showed was confined to below 1500 m altitude.

Wilson (1979) analysed anemometer data taken on a 390 m tall tower over flat coastal terrain at North West Cape in Western Australia, during four decaying tropical

cyclones between 1973 and 1977. He argued that the roughness length differences between sea and land were small in this case, so that the profiles could be regarded as not being substantially modified by internal boundary layer effects. The overland fetch varied between 4 and 50 km, depending on wind direction. The profiles often showed a wind-speed maximum between 60 m and 200 m, which was more pronounced closer to the storm centre. The profile shape was also somewhat dependent on storm quadrant, with some suggestion that the jet was lower to the right of the (Southern Hemisphere) storms, and stronger towards the front of the storm.

May et al. (1994) presented data from 915 MHz and 50 MHz wind profiling radars situated on Saipan, as Tropical Storm Flo passed nearby. There was some evidence of a low-level wind maximum, particularly at and immediately before the time of closest approach when it was at a height of about 1 km. The track was towards the west-northwest and passed 115 km to the south of Saipan; thus the observations represent a section through the right hand side of the storm.

Marks et al. (1999) presented horizontal wind analyses, derived using the velocity-azimuth display (VAD) technique from de-aliased WSR-88D Doppler radar data, as the low category-three Hurricane Fran made landfall 25 km to the east of the radar. The observations show a marked speed maximum near 2 km, which decreased in height as the storm approached, to about 1.3 km at the closest approach. The wind direction was nearly constant below 450 m, and turned by approximately 50^{o} in the 1.5 km above that. Their radius-height section of radar reflectivity, azimuthal and radial winds, reproduced here as Fig 1.11, shows inflow is a maximum at 200 to 500 m, with the maximum values on the outer edge of rainbands. Maximum azimuthal winds lie in the outflow region at about 2 km; however the maximum outflow is always above the

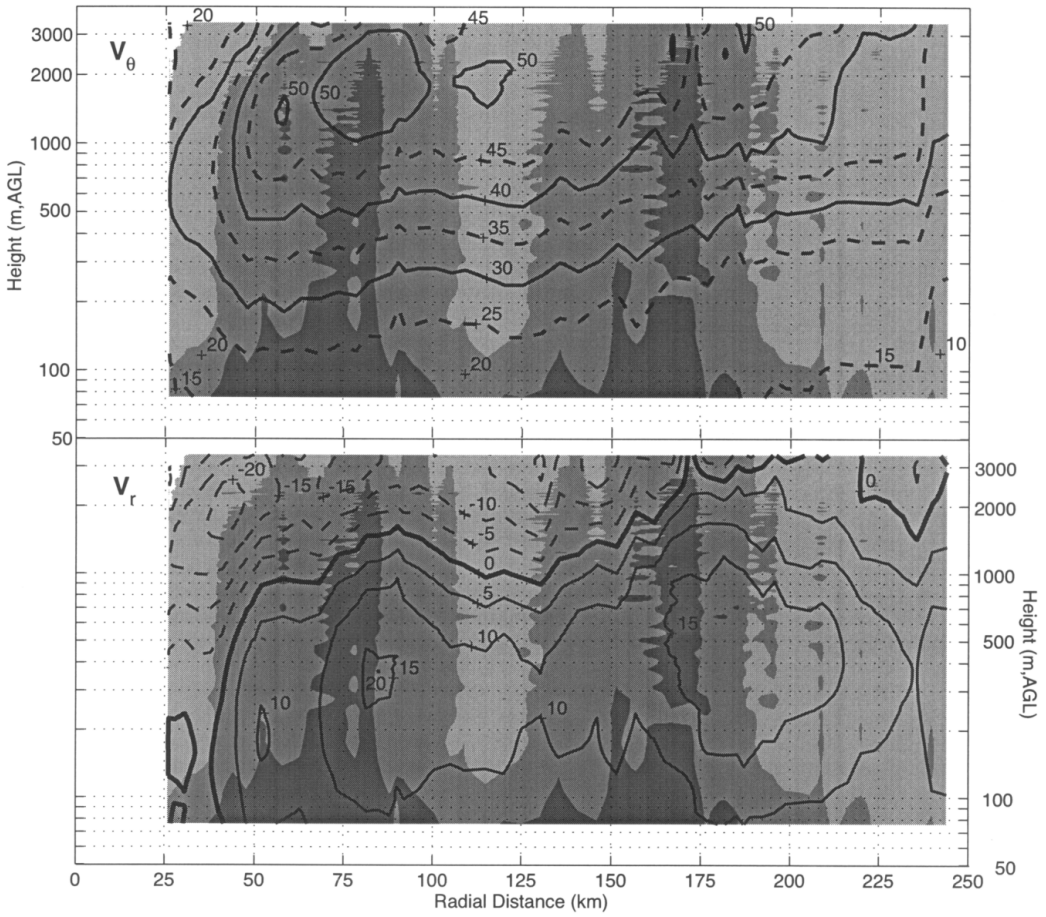

Figure 1.11 Radius-height sections of radar reflectivity (shading), azimuthal (top) and radial (bottom) winds, as determined from Doppler radar data using the VAD technique during Hurricane Fran by Marks et al. (1999).

azimuthal wind maximum. The heights of the azimuthal, outflow and inflow maxima all decrease towards the centre of the storm.

The measured profiles discussed above are all limited in some way by the observation technique. For instance, direct aircraft observation is unsafe too near the surface or in regions of intense convection or very high wind speed. Doppler radar observations involve volume averaging and are subject to sea clutter near the surface. Tall tower observations must wait for a cyclone to pass, and are land-based. Many of these limitations are overcome by the recent development of the GPS dropsonde, which provides observations of wind speed and direction, pressure, temperature and humidity with a vertical resolution of approximately 5 m in the lower troposphere, and accuracies of 0.5 m s^{-1}, 0.5 hPa, 0.2 ^{o}C and 2 %, respectively (Hock and Franklin, 1999). So far little of the resulting wealth of data has been analysed; an example shown here as Fig 1.12 was taken from the cover of the Hurricane Research Division's 1998 Field Plan. This shows three wind speed profiles in the eyewall of Hurricane Guillermo of 1997. It is noteworthy that in two cases the surface wind speed is close to that at 1500 m, and that two of the profiles show broad wind-speed maxima below 1 km, together with marked smaller scale structure. This low-level wind maximum was briefly discussed by Black and Shay (1998).

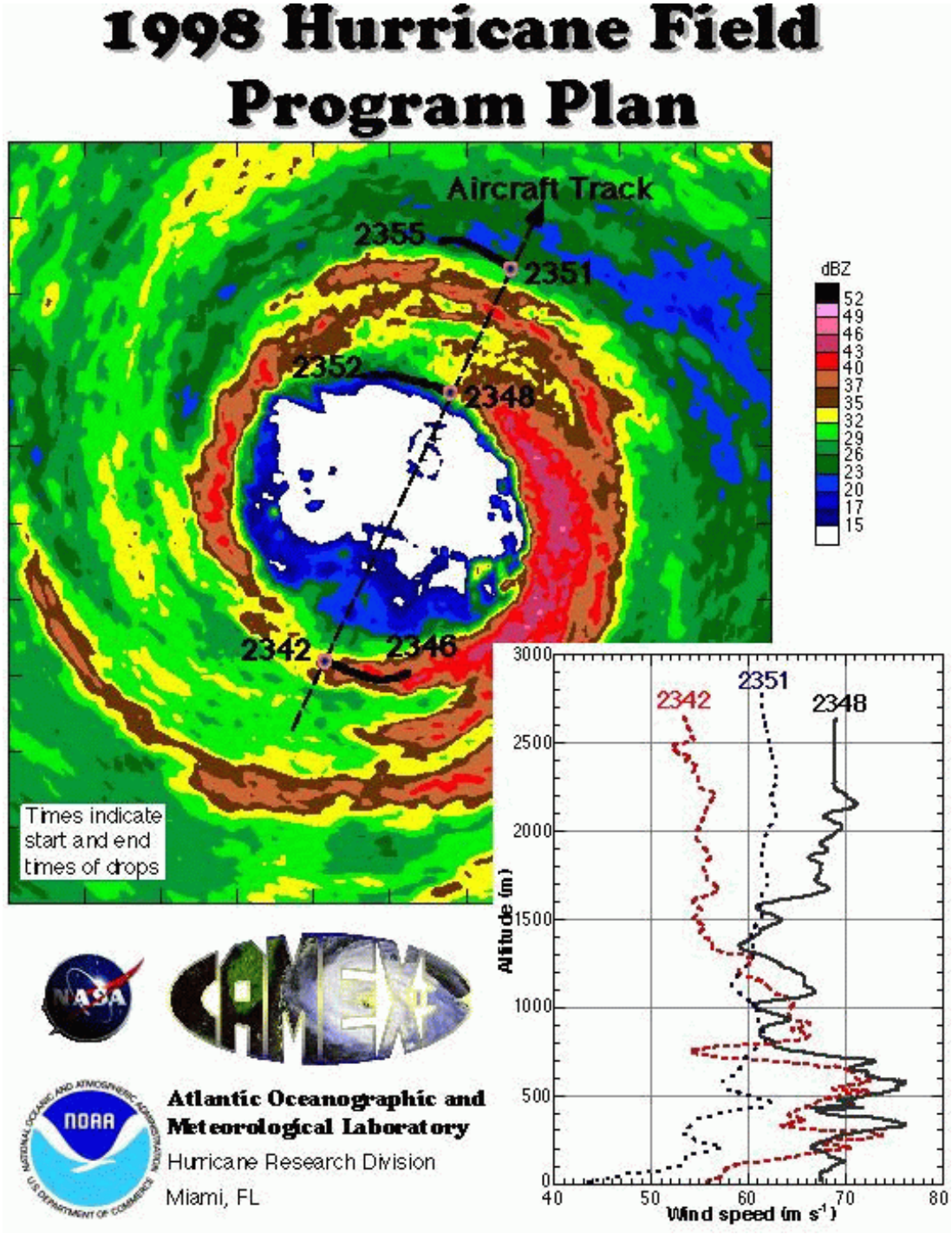

Figure 1.12 The cover of the Hurricane Research Division's 1998 Hurricane Field Plan, showing three wind speed profiles measured in the eyewall of Hurricane Guillermo by GPS dropsondes, together with a radar reflectivity image with the dropsonde trajectories superimposed.

1.2.4 Coherent structures in the tropical cyclone boundary layer

The final phenomenon to discuss is that of boundary layer rolls. These are frequently present in the atmospheric boundary layer, particularly under conditions of unstable stratification. They consist of horizontal roll vortices aligned more-or-less with the geostrophic flow, with a spacing typically from 4 to 6 times the boundary layer depth, although this can be as low as 2 or as high as 15. The most spectacular manifestation is when they lead to cloud streets. Further details can be found in the review of Etling and Brown (1993). Two recent observational studies present evidence, albeit somewhat conflicting, for the existence of boundary layer rolls in hurricanes. Wurman and Winslow (1998) used high-resolution data obtained by a portable Doppler radar during the landfall of Hurricane Fran in 1996 to show that the flow below 500 m consisted of bands of intense winds of 40 to 60 m s^{-1} alternating with much weaker flow of 15 to 35 m s^{-1}. Above 500 m, the flow was relatively uniform at 50 to 60 m s^{-1}. The bands were found to be aligned approximately parallel to the larger scale flow and to the surface to 1000 m shear vector, with a highly variable horizontal spacing, which averaged about 600 m.

The study of Gall et al. (1998) utilised data from conventional and Doppler weather-watch radars in three hurricanes at landfall. Spiral bands with a spacing of approximately 10 km, and depth of 5 to 6 km, were visible in both reflectivity and velocity data once the larger scale features had been filtered out. The bands were up to 100 km long, moved with the tangential wind, and took the form of equiangular spirals with a crossing angle of approximately 10°. In cases where both reflectivity and velocity data were available, it was found that the enhanced reflectivity was associated with stronger winds, and (from aircraft data) with higher equivalent potential temperature. They speculated that the observed rolls may be the result of an instability similar to that in the more usual boundary layer rolls, with some modification due to latent heat release.

Given the different scales, it is possible that these two studies are presenting different phenomena. They could well coexist – although given that the rolls observed by Wurman and Winslow (1998) were restricted to be very near the surface, and were below the spatial resolution of conventional weather-watch radar, proving this could be difficult. To date the questions of how common these bands are, and what conditions favour their formation, are unanswered. If, however, they are a reasonably common occurrence, they are likely to play as important a role in vertical transport within a tropical cyclone as their more benign counterparts do within the atmospheric boundary layer.

1.2.5 Final remarks on observational studies

In summary, the observational studies show that the maximum boundary layer wind speeds are most often found on the right hand side of the storm in the Northern Hemisphere. There is some suggestion that this maximum may rotate with height through the right forward quadrant to be nearer the front of the storm at the surface. The storm-relative radial flow generally consists of inflow in the right rear and outflow at the left front, or in stationary coordinates inflow from the right front and outflow in the left rear. In combination, these lead to an inflow angle (for the earth-relative flow) that is a maximum to the right rear of the storm, and a minimum to the left front, where outflow is possible. The horizontal convergence near the surface is typically largest ahead of the storm and near the RMW. A region of horizontal divergence may extend from the centre of the storm into the left rear in the upper boundary layer. This usual situation is shown schematically in Fig 1.13. However, distributions of wind other than this are possible, for example when the storm is embedded in strong environmental shear.

Vertical profiles show that a boundary-layer wind speed maximum is a common

feature, with the reported height varying between 60 m and 1.5 km. Where several profiles at different radii in the one storm are available, they show that the height of the maximum tends to decrease toward the storm centre. The ratio of wind speed aloft to that at 10 m was found to vary from about 0.55 to (or even slightly above) 1. There was also ample evidence that this varied with stability, with the lowest (highest) values being observed when the sea was cooler (warmer) than the air.

One multilevel study had sufficient data to analyse both the symmetric and asymmetric flow components at several heights within the boundary layer. This showed that the depth of the former decreased rapidly towards the centre of the storm, while the latter decays more slowly, and rotates anticyclonically, with height.

Two studies found evidence of roll vortices aligned approximately with the mean boundary layer wind. One of these was quite confined in vertical extent, and seems consistent with the rolls observed elsewhere in the atmospheric boundary layer. The other had a depth rather greater than that of the boundary layer, and is probably a distinct phenomenon.

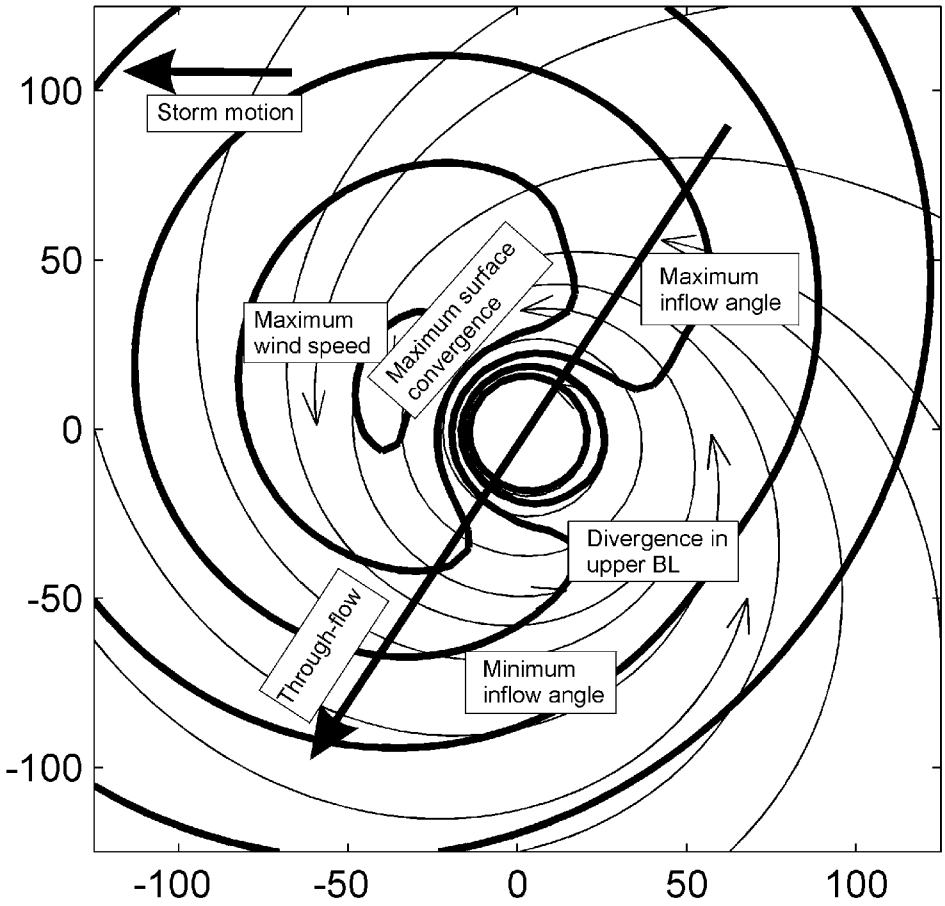

Figure 1.13 Schematic streamline-isotach analysis of the near-surface earth-relative flow in a typical northern hemisphere tropical cyclone, moving to the left of the figure, with axes labelled in kilometres. The strongest wind speed is found in the right forward quadrant, while inflow is a maximum in the right rear. Similarly, the inflow angle is markedly asymmetric, being a maximum towards the rear, and a minimum to the left of the storm. The overall asymmetry in the azimuthal and radial flow components can be approximated as a through-flow from right rear to left front. While this is the most common situation, other distributions are possible.

1.3 Theoretical and Modelling Studies of Tropical Cyclone Boundary Layer Wind Structure

Through the 1960's and first part of the 1970's, a number of theoretical studies of the tropical cyclone boundary layer appeared. These were motivated partly by a desire to better resolve the low-level radial inflow, since this forms a large part of the cyclone's meridional circulation and hence plays a crucial role in the storm's overall energy and angular momentum budgets (e.g. Rosenthal 1962). Observational studies, as discussed above, had not succeeded in describing it adequately at that time, because of the inherent difficulty of taking observations there, and also that small aircraft navigation errors produced relatively large errors in the derived radial component. A second motivation was to improve the parameterization of the surface boundary condition in numerical models of tropical cyclones, particularly given the very coarse vertical resolution prescribed by the computers of the time (e.g. Anthes, 1971). A related problem was the requirement for a lower boundary condition in efforts to diagnose the secondary circulation from the observed azimuthal flow (e.g. Krishnamurti 1961, 1962, Estoque 1962, Barrientos 1964). Thus it was hoped that better knowledge of the boundary layer would lead to both improved understanding of cyclone energetics, and to numerically affordable parameterisations to support the growing numerical modelling effort.

A further important question was the distribution of the updraft. The prediction of classical Ekman theory, that the vertical motion at the top of the boundary layer was proportional to the curl of the surface stress, was contradicted by the available observations in tropical cyclones. Did the boundary layer play a role in organising the eyewall updraft, or the subsidence in the eye? Interest thus focussed not only on determining the net frictionally forced mass circulation, but also on how the updraft was distributed.

1.3.1 The Ekman Spiral

The oldest and probably best known model for geophysical boundary layers is the Ekman spiral, originally proposed by Ekman (1905). A large literature has developed since, which this brief discussion does not attempt to review. A good introduction may be found in Haltiner and Martin (1957, pp 233-242), and a more thorough treatment in Brown (1974). Rather, the aim is to touch on several issues that will be relevant later in this thesis.

In its original form, and as presented in many textbooks and monographs since, the Ekman spiral utilises a no-slip surface boundary condition, with a constant turbulent diffusivity above. This tends to predict near-surface winds which are rather lighter than observed, with too large a surface cross-isobar flow angle, and too high a surface stress. Many studies have extended the basic theory by incorporating the effects of flow curvature, baroclinicity, more realistic diffusivity profiles including the effects of stability, etc, but will not be discussed here. Two important improvements will, however, be briefly discussed.

Taylor (1915) solved the Ekman equations with a semi-slip surface boundary condition, in which the surface stress was aligned with the near-surface wind. He introduced an additional parameter, the cross-isobar flow angle, to close the system and derived a relationship between this and the surface wind speed which showed much better agreement with observations than could be obtained from the no-slip condition. He also compared model and observed mean wind profiles over the Salisbury Plain in which he restricted attention to wind speeds over 13 $m\,s^{-1}$. Translating his argument into modern language, this was so that the shear production of turbulent kinetic energy dominated the diurnally varying buoyant production, so the diffusivity profile was

relatively simple in form and constant in time. He showed remarkably good agreement between observations and theory in this case.

Ekman (1928) considered a two-level model with constant diffusivities in each layer, being a thin near-surface layer with small diffusivity and a thicker layer aloft with higher diffusivity. This produced profiles similar to Taylor's, a key point being that the use of a smaller diffusivity near the surface reduced the cross-isobar component there and hence improved the agreement with observations. It is easily shown that the cross-isobar mass transport in an Ekman-like spiral is proportional to the surface stress (e.g Gill 1982, p 321). Thus the reduced surface stress in the two-layer model allowed stronger winds near the surface and reduced cross-isobar flow, in better agreement with observations. Note also that Prandtl's (1925) parameterisation[3] of diffusivity within the surface layer $K = k\, u_* \, z$, where $k = 0.4$ is von Kármán's constant, u_* is the surface friction velocity and z is the height, yields a logarithmic wind profile with constant stress. This stress could be applied as a semi-slip surface boundary condition to the Ekman equations by the usual bulk formula with drag coefficient defined by $C_D = (u_*/u)^2$, where u is the wind speed at some fixed reference height within the surface layer. Thus the wind profile predicted by Ekman's (1928) two-layer model is similar to that of Taylor (1915).

Prompted by observations of the atmospheric boundary layer showing rolls aligned approximately along the flow, Faller and Kaylor (1966), Lilly (1966), Brown (1970) and others showed that the basic Ekman profile was unstable. The instability lead to the development of rolls aligned at a small angle to the mean flow. The additional momentum transport by the rolls modified the mean wind profile so that it was more

[3]See Garratt (1992, p 40) or Schlichting and Gersten (2000, p 537-538 and 557-558) for further discussion.

closely aligned with the geostrophic flow, and had a more strongly supergeostrophic region in the upper boundary layer. The instability grew most strongly when the rolls were aligned about 18 degrees to the right of the geostrophic wind, although there was a secondary maximum at very high Reynolds number for rolls aligned 5 degrees to the left of the flow. Brown (1972a) extended this theory to include the effects of static stability and found that under unstable conditions the rate of growth of the instability was increased, that the rolls were more closely aligned with the wind direction and were of shorter wavelength. Conversely, stable stratification tended to damp the instability. Physically, the instability arises because of the inflection point in the Ekman lateral velocity, which gives rise to a mid-boundary layer maximum in the along-stream vorticity component. The instability in the lateral flow is thus similar to Kelvin-Helmholtz instability (Brown, 1972b). An important consequence of this is that any boundary-layer wind profile with an inflection point in the lateral component is unstable; that is, the instability is not peculiar to the Ekman spiral. As well as reducing the cross-isobar angle, Brown's results show an increase in the wind speed at 100 m, relative to the Ekman spiral. Thus his results show improved agreement with observations, even though he used a no-slip surface boundary condition.

Probably the state-of-the-art in the family of Ekman models appears to have been first derived by Rossby and Montgomery (1935), then rediscovered by many others including Brown (1981). These match a logarithmic surface layer in which K increases linearly with height to a constant diffusivity Ekman spiral above. Velocity, shear and diffusivity are continuous at the matching height. The profile modifications due to baroclinicity, stability and longitudinal rolls are included in Brown's (1981) model.

1.3.2 Axisymmetric models of tropical cyclone boundary-layer structure

The first significant advance was an Ekman-like model of the boundary layer flow in a symmetric hurricane, developed by Rosenthal (1962). He used a semi-slip boundary condition, and linearised about the gradient flow. The results were applied to an idealised radial pressure profile typical of those observed. The depth of the boundary layer was shown to decrease markedly towards the RMW. The difference between near-surface azimuthal wind and the gradient wind was nearly constant outside the RMW, but decreased to zero inside; thus the predicted surface winds on the inner side of the RMW were close to gradient-wind strength. The inflow was a maximum at about twice the RMW, near the surface. Although the horizontal convergence increased rapidly towards the centre, to be a maximum just inside of the RMW, the decrease in the boundary layer depth at the RMW limited the vertically integrated horizontal convergence, with the updraft at the top of the boundary layer being 0.23 m s^{-1}. This was argued by Rosenthal to be too weak, and so he concluded that the decrease in boundary layer depth towards the centre was not realistic. He suggested that making the diffusivity increase towards the centre, rather than being radially constant, would improve the results.

Miller (1965) applied Rosenthal's (1962) model with a diffusivity chosen to make the boundary layer depth radially constant. This increased the maximum updraft to 0.36 m s^{-1}, an improvement, but which he suggested was still too small. He also presented an axisymmetric numerical model which included processes neglected in the Rosenthal model, including the vertical advection and horizontal diffusion, and the full nonlinear horizontal advection terms. The horizontal diffusion coefficients used varied from 1.5×10^4 m^2s^{-1} to 3×10^5 m^2s^{-1}; by modern standards these are very large. The full model produced changes in the detail of the solution from that found by Rosenthal (1962); in particular the maximum inflow moved inwards and the eyewall updraft slightly

strengthened. Very slightly supergradient winds were found in the upper boundary layer.

Anthes (1971) presented numerical solutions to the boundary-layer flow beneath an imposed hurricane-like pressure field, using the full nonlinear dry Boussinesq equations. He used nine levels in the vertical, with the upper level at 850 m, and one aim was to compare the predictions of this high resolution model with a single-level model, which was similar to the then typical resolution within the boundary layer of full numerical models. A further focus was on the sensitivity to the horizontal diffusion, and coefficients ranging from 5×10^4 m^2s^{-1} to 2.5×10^5 m^2s^{-1} were employed. These large values were justified partly by a scale analysis based on the notion that the horizontal diffusion of inflow in the radial flow budget equation should be of similar magnitude to the centripetal acceleration. The updraft generally lay on the inside of the RMW, and weakened slightly and moved inwards as the horizontal diffusivity increased. As the drag coefficient or vertical diffusivity were increased, the maximum updraft strengthened and moved inwards. However, the changes were not large (over the range tested) and the peak updraft in all cases presented was approximately 0.5 to 0.6 m s^{-1}. The relative magnitude of the terms in the radial momentum equation at two levels and several radii were tabulated. This showed that the flow was strongly supergradient inside the RMW, since the centripetal acceleration was up to several hundred times that of the pressure gradient there. These large values were balanced by horizontal diffusion near the surface, and vertical and horizontal diffusion at the upper level. The only exception was for a more weakly supergradient flow just inside the RMW at a height of 750 m. Here the diffusion terms were much too small (and of the wrong sign) to give balance, which was obtained predominantly from the vertical advection of inflow.

Smith (1968) applied a momentum integral technique to diagnose the boundary-

layer properties. The shape of the boundary-layer wind profiles were assumed, and differential equations for the boundary-layer scale-depth and the magnitude of the inflow were solved by numerically integrating inwards from some large radius. The boundary-layer depth decreased markedly towards the centre, and a strong updraft occurred near the RMW. This was stronger than Rosenthal (1962) found, at least partly because Smith's use of a no-slip surface boundary condition overestimated the surface stress and hence the cross-isobar flow. Subsequent refinements, including a better representation of the surface boundary condition, the use of a radially varying diffusivity, and the correction of an error, (Leslie and Smith 1970, Bode and Smith 1974) gave an updraft of similar magnitude to Rosenthal's. However, the momentum integral technique was unable to precisely locate the position of the eyewall updraft due to the violation of an assumption near the RMW.

Kuo (1971) modified the momentum integral technique to iteratively calculate the boundary layer wind profiles, rather than simply assuming their form as above. (Bode and Smith (1974) objected to this extension.) Kuo found that the vertical velocity was proportional to the square root of the cyclostrophic vorticity (he neglected the Coriolis force since he was primarily interested in tornadoes) in the core of his vortex, and was weakly downwards in the outer part where the radial gradient of angular momentum was approximately zero. The wind profiles in the outer part of the vortex, where the weak downdraft prevailed, showed a deep boundary layer with a monotonic decrease in azimuthal component towards the surface, while the inflow increased steadily to a maximum at or near the surface. Closer to the core, where an updraft existed, the character of the solutions changed markedly. The radial flow took the form of alternating layers of steadily weaker inflow and outflow as height increased, while the azimuthal flow consisted of similarly alternating layers of sub- and super-cyclostrophic flow. The

depth of the boundary layer markedly decreased as the transition from downdraft to updraft was made, and the thickness of the oscillating layers continued to decrease towards the centre. Kuo (1982) repeated this study with a different mathematical technique and the inclusion of the Coriolis terms, and obtained similar results.

Eliassen (1971) made an important advance in understanding the conditions in the eye when he considered the Ekman layer developed beneath a circular vortex in solid-body rotation, using both no-slip and quadratic drag law surface boundary conditions. For the former case, he found that the updraft at the top of the boundary layer was independent of radius, in accordance with the earlier results of Greenspan and Howard (1963). However, the quadratic drag law produced the remarkable result of an updraft that was zero at the centre, and increased linearly with radius. As his vortex was in solid-body rotation, this result is only applicable in the eye of a tropical cyclone. But it appears from this that the boundary layer could have a controlling influence on the location of the updraft in which the all-important latent heat release takes place. Moreover, the very large change in the distribution of the updraft found when the no-slip boundary condition was replaced by the semi-slip one suggests that the model boundary layer, and particularly the inflow, is substantially in error when the no-slip condition is used.

This study was extended to include the outer flow of a more realistic circular vortex by Eliassen and Lystad (1977), who also calculated the spin-down time of such a vortex. They filtered the equations of motion to exclude inertial oscillations, by eliminating the radial and vertical advection terms. A heuristic analysis for a linearised equation set repeated the earlier results on updraft forcing within the RMW, and also showed that the quadratic drag law led to an algebraic spin-down of the vortex, with the

decay half-life being inversely proportional to radius. On the other hand, the no-slip condition led to a spatially uniform, exponential decay. The heuristic analysis also reproduced Rosenthal's (1962) boundary layer depth scale $(2K/I)^{1/2}$, and gave an estimate for the time scale for formation of the Ekman layer of $1/I$. The filtered nonlinear equations were then numerically integrated, starting from a condition of vertically uniform motion, for a variety of surface drag coefficients and vortex Rossby numbers. Results were in excellent agreement with the heuristic analysis and also showed many features of Rosenthal's (1962) work. In particular, the Ekman spiral resulted in weakly supergradient flow in the upper boundary layer, with weak outflow aloft and inflow below; maximum inflow was near the surface and outside the RMW; and the depth of the inflow decreased towards the centre. In addition, the maximum updraft was always within the RMW, and generally moved outwards as the vortex Rossby number increased, and inwards as the drag coefficient increased.

The Eliassen and Lystad model was revisited by Montgomery et al. (2001), who used a full axisymmetric Navier-Stokes model to verify the theory for a hurricane-strength vortex. (Eliassen and Lystad's most intense vortex had a maximum wind speed of only 10 m s^{-1}.) One finding was that the spin-down in the full model occurred slightly faster than the Eliassen-Lystad theory suggested; this was because of the formation of a thin region of outflow immediately above the Ekman layer that was not predicted by the theory. There was also a tendency for the vortex to intensify slightly for the first part of the integration. Predictions of spin-down rate from the theory were compared to observed decay rates for two weakening hurricanes, with reasonable agreement.

Carrier (1971) and McWilliams (1971) presented analyses of the boundary-layer flow beneath vortices of various forms. Since they used the no-slip surface boundary

condition, their results must be interpreted with care. However Carrier performed two calculations which are relevant here. The first was to introduce an approximate form of the vertical advection, where w is constant with height, to the vortex in solid body rotation. The updraft remained spatially uniform, but both it and the inflow were strengthened. The other was the consideration of a vortex with frictionless flow given by $V(r) = A/r(1 - (r/r_0)^2)$ for constants A and r_0; that is, approximately potential flow but going to 0 at $r = r_0$. This is applicable to tropical cyclones, if we take r_0 = 1000 km, A such that V(40 km) = 40 m s^{-1}, K = 50 m^2 s^{-1} and $f = 3\times10^{-5}$ s^{-1}. Carrier considered two limits, for small and large r. For large r, which here means greater than about 200 km, the vertical motion at the boundary layer top $w_\infty = -A/r_0^2(\nu/2f)^{½} \sim -1.5$ mm s^{-1}; that is, a weak downdraft. For small r McWilliams corrects Carrier's result[4] to be a downdraft proportional to $-1/r$. For a tropical cyclone scale vortex, the approximation is less accurate for small r than large, and this wind profile is considerably more peaked than in Shea and Gray's (1973) average of $V \sim r^{-0.5}$. Even so, the finding that the vertical motion in such a vortex is downwards, and increasingly so towards the core, is intriguing. McWilliams (1971) also considered the potential vortex, and found similarly that w_∞ is always downwards, approximately constant at large radii, but increasing rapidly towards the core.

[4] Carrier added a footnote in proof which corrects his algebraic error, but regrettably omits a minus sign.

1.3.3 The horizontal structure

Shapiro (1983) used a slab model to calculate the depth-averaged boundary flow beneath a hurricane. He assumed a constant boundary-layer depth, applied a quadratic drag law for the surface boundary condition with a wind-speed dependent drag coefficient, and presented numerical solutions to the full equations of motion (except vertical advection) in cylindrical coordinates, forced by a known symmetric pressure field similar to that in a hurricane. For a stationary hurricane, he found that inflow increased steadily inwards to the RMW, before decreasing rapidly as it impinged upon the "inertial wall" immediately inside. The resulting strong convergence produced a strong updraft just inside the radius of maximum gradient winds, and the boundary-layer azimuthal flow peaked and was supergradient just inside the gradient RMW, due to "overshooting" of the inflowing air.

The greater part of Shapiro's paper, however, was devoted to the analysis of the flow beneath a moving hurricane, and his was thus the first theoretical study to consider the motion-induced asymmetry in detail. He expanded the azimuthal variation in the boundary layer flow as a Fourier series, truncating at wave-number two. Separate budget equations were derived for each Fourier component, including the explicit wave-wave (nonlinear) interaction terms. His results are reproduced here as Fig 1.14. The inflow is strongest to the right front of the vortex, and somewhat inside of the gradient RMW. The resulting strong advection of angular momentum places the strongest winds just inside and downstream of this; relative to the earth the winds in the right front are stronger than those in the left front, but the situation is reversed relative to the vortex. This implies a quite marked inwards tilt of the RMW at the front of the hurricane. The maximum convergence and updraft follow a broad arc very close to the strongest winds.

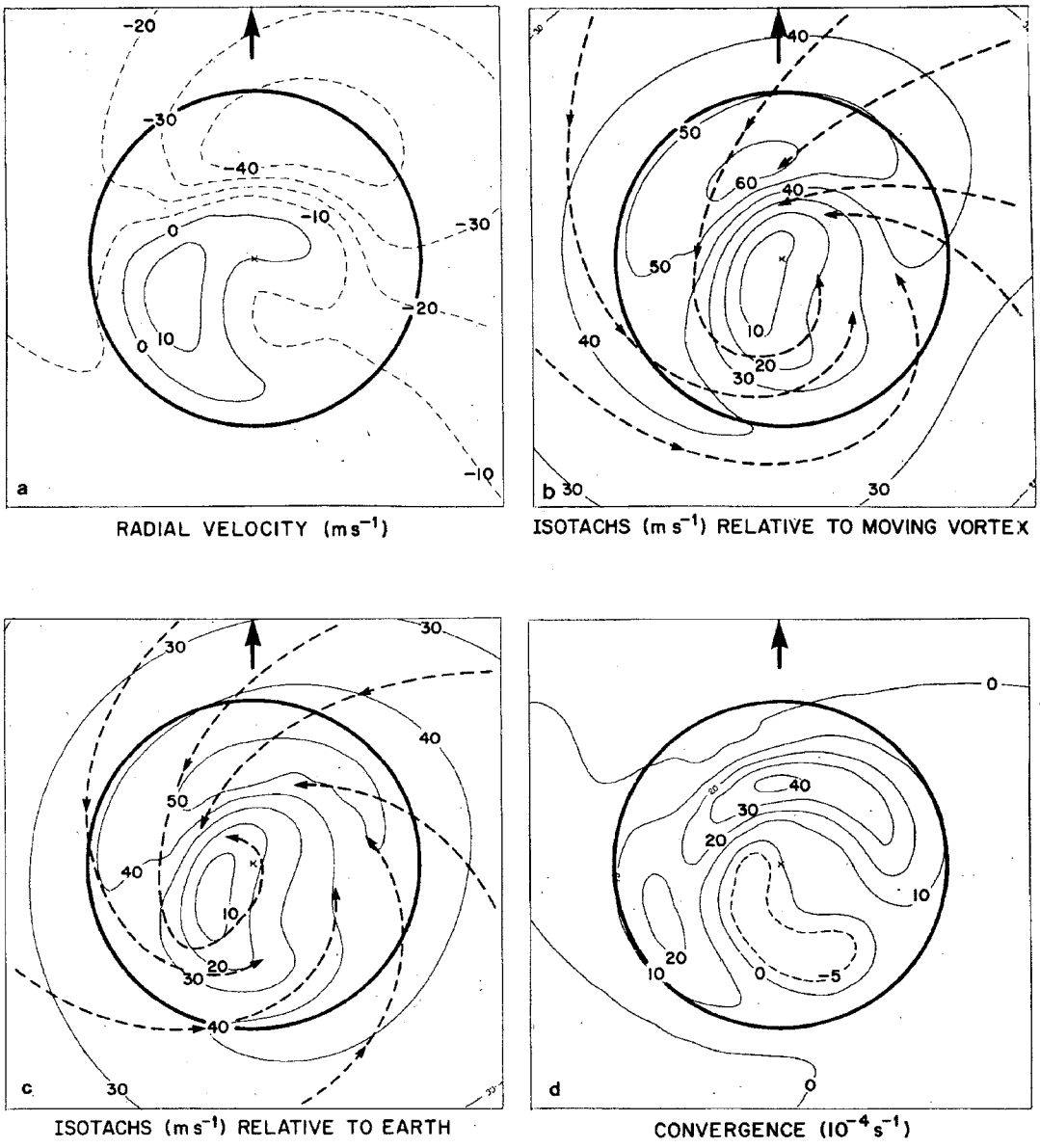

Figure 1.14 Mean boundary-layer flow, as modelled by Shapiro (1983) for a cyclone translating towards the top of the page at 10 m s^{-1}. The circle indicates the radius of maximum gradient wind. Top left: Storm relative radial flow. Top right: Storm relative streamlines and isotachs. Lower left: Earth relative streamlines and isotachs. Lower right: Horizontal convergence.

The various budget equations and in particular the interactions between the Fourier components were analysed in considerable detail by Shapiro. For a slow-moving vortex, these are comparatively weak and the storm-relative winds are strongest to the left. Convergence is large in a broad arc ahead of the storm, and there is divergence within the nearly circular eye. As the translation speed increases, the nonlinear interactions between Fourier components become important, leading to inflow and convergence becoming concentrated ahead of the storm, a more elliptical eye and a contraction of the boundary layer RMW.

Vickery et al. (2000) similarly considered a depth-averaged model, but numerically represented their equations using finite differences on a Cartesian grid, rather than the semi-spectral approach of Shapiro (1983). At low to moderate translation speeds, their results are indistinguishable. At high translation speeds, the maximum tended to move inwards, and to the right of the storm. They also showed that in this latter case, the spectral truncation at azimuthal wave-number two by Shapiro led to inaccurate results.

1.3.4 The Deardorff-Moss-Rosenthal-Powell Wind Profile Model

The profile model of Deardorff (1972a) was originally formulated to provide an economical parameterisation of the boundary layer for use in general circulation models, and was subsequently extended and applied to the tropical cyclone boundary layer (Moss and Rosenthal 1975, Powell 1980, Powell et al. 1996). It has been widely used to estimate near-surface winds from aircraft observations, typically taken at 500 m or higher. As many of the observational analyses of surface wind fields discussed in the previous section rely on its use, it is appropriate to review its formulation and briefly discuss its relevant properties.

The model comprises two matched layers. The surface layer parameterisation uses Monin-Obukhov similarity theory with the stability functions of Businger et al. (1971), while the mixed layer is based on the "deficit laws" which Deardorff (1972b) had derived from his large-eddy simulations. Both layers use the Monin-Obukhov length as an internal stability parameter, with the bulk Richardson number being an additional stability parameter to the mixed layer part of the model. The matching requires that the profiles of wind speed and thermodynamic variables be continuous at the top of the surface layer, which is assumed to be 1/40 of the boundary layer depth. The input parameters are thus the boundary layer depth, mean potential temperature, mean specific humidity and mean wind, the surface temperature and moisture, and the roughness length. Deardorff (1972a) also included some discussion of how to determine the boundary layer height. The parameterisation was developed particularly to give the surface fluxes and related quantities, but other internal variables, such as the anemometer-level wind, are also available.

Moss and Rosenthal (1975) extended the Deardorff (1972a) model to include a

wind speed dependent surface roughness length, using either the Charnock (1955) or Cardone (1969) formulation. This necessitated an iterative solution for the friction velocity. The boundary-layer depth was diagnosed as the lifting condensation level (in lieu of Deardorff's prognostic equation), and the resulting model applied to data from Hurricanes Daisy of 1958 and Inez of 1966. Their analysis concentrated on the comparison of the bulk transfer coefficients from the model with those calculated from budget studies and empirical formulae. They found generally good agreement for the drag coefficient compared to those obtained from budget analyses, a remarkable result given that this application involved extrapolation of the parameterisations to much higher wind speeds than those for which they had been developed, and the considerable uncertainties inherent in the budget studies. On the other hand, the model overestimated the heat transfer coefficient (relative to the one budget study available), which may have been due to its use of the same roughness length for heat and momentum.

The Deardorff-Moss-Rosenthal (DMR) model was one of several tested on a small amount of nearly co-located aircraft and buoy data by Powell (1980). As already mentioned, three of these models gave agreement within 10% of observations. The best performers were DMR, a modification of DMR by Powell (1980)[5] (henceforth DMRP), and a model of Cardone (1969), which applied surface layer similarity theory to the entire layer from the surface to flight level. Subsequently, the DMRP model has been

[5]The main differences were the addition of a final step to calculate the 10 m wind from the derived surface layer parameters, rather than simply using the wind at the assumed surface layer top of 1/40 the boundary layer depth, and the use of the Charnock roughness length (with coefficient 0.035, and later 0.0144) rather than that of Cardone (1969). The results from the DMR and DMRP models in Powell's (1980) paper are very similar.

extensively used for research and more recently operations, to "reduce" flight-level observed winds to the surface. Further details and some recent modifications to the model are given by Powell et al. (1996). These include changing Businger et al.'s (1971) von Kármán constant and turbulent Prandtl numbers of 0.35 and 0.74 to the now more widely used 0.4 and 1.0, respectively. The scheme's formulation and properties are now briefly outlined.

Deardorff (1972a) eliminated the anemometer-level wind and virtual potential temperature between the surface-layer similarity equations and his deficit laws. He thus wrote equations for momentum and heat-transfer coefficients C_D and C_H,

$$C_D^{-1} = \frac{u_m}{u_*} = F\left(\frac{h}{z_0}, \frac{h}{L}\right) \qquad \textbf{(1.1)}$$

and

$$C_H^{-1} = \frac{(\theta_{vm} - \theta_{vs})}{\theta_*} = G\left(\frac{h}{z_0}, \frac{h}{L}\right) \qquad \textbf{(1.2)}$$

where the subscript m refers to the boundary-layer average, h is the boundary-layer depth, L the Monin-Obukhov length, F and G were given functions, and other symbols have their usual meanings. Note that these differ from the more usual forms $C_D = (u_*/u)^2$ and $C_H = (\theta_*/\Delta\theta)(u_*/u)$. These were combined to give an equation for the bulk Richardson number in terms of h/z_0 and h/L, which could be solved numerically to give the unknown h/L, and thus u_*, θ_{v*} and hence the fluxes. Deardorff gave approximate fitted curves for C_D and C_H; here we confine attention to C_D. For neutral conditions,

$$C_{DN} = \left(k^{-1} \log\left(\frac{0.025h}{z_0}\right) + 8.4\right)^{-1} \qquad \textbf{(1.3)}$$

with stability corrections

$$C_D = \begin{cases} [C_{DN}^{-1} - 25\ \exp(0.26\xi - 0.03\xi^2)]^{-1}, & \mathrm{Ri_B} < 0 \\ C_{DN}\ (1 - \mathrm{Ri_B}/\mathrm{Ri_C}), & \mathrm{Ri_B} > 0 \end{cases} \qquad \textbf{(1.4)}$$

where

$$\xi = \log_{10}(-\mathrm{Ri_B}) - 3.5 \qquad \textbf{(1.5)}$$

and $\mathrm{Ri_B}$ and $\mathrm{Ri_C} = 3.05$ are the bulk and the bulk critical Richardson numbers. Powell (1980) then used the familiar

$$u(z_a) = \frac{u_*}{k}\left(\log\left(\frac{z_a}{z_0}\right) - \psi_m\left(\frac{z}{L}\right)\right) \qquad \textbf{(1.6)}$$

where ψ_m is the stability function for momentum (see for example Garratt, 1992, page 53) with the parameter values recommended by Dyer (1974), to give the 10-minute mean wind speed at anemometer-level z_a. This could in turn be adjusted to a 1-minute sustained wind by multiplying by 1.12 (Powell et al., 1996).

In neutral conditions, (1.1), (1.3) and (1.6) are easily combined to give a formula for the surface-wind ratio:

$$\frac{u(z_a)}{u_m} = \frac{\log(z_a/z_0)}{\log(0.025h/z_0) + 8.4k} \qquad \textbf{(1.7)}$$

For reduction of aircraft winds to the surface, this is applied with u_m the observed wind speed, $h = 500$ m and $z_a = 10$ m. Thus in neutral conditions over the land the surface-

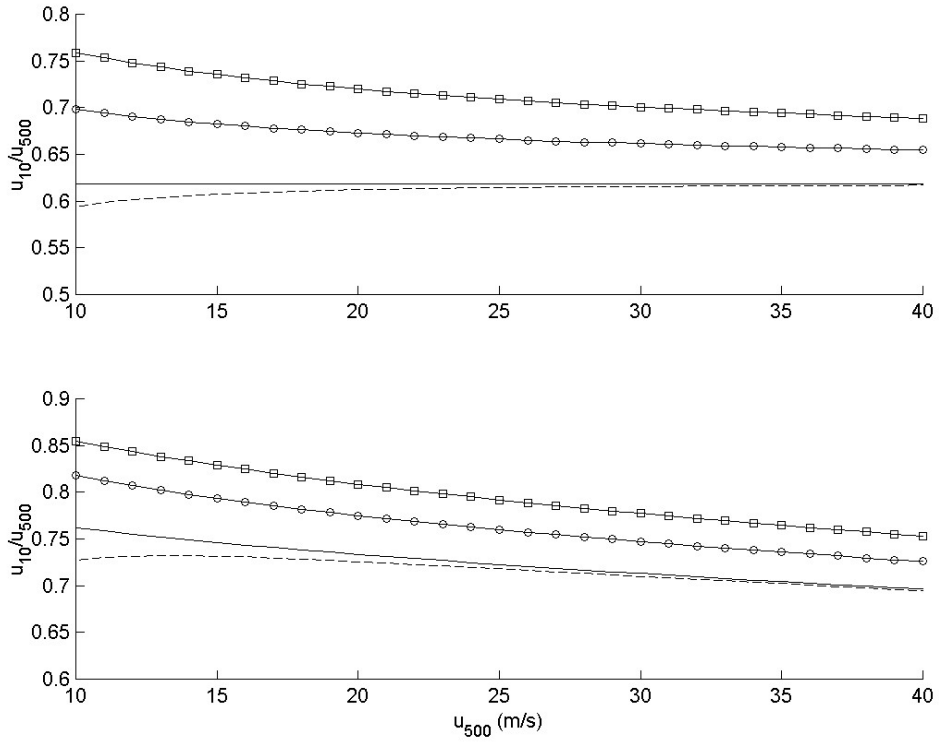

Figure 1.15 Surface wind ratios predicted by the DMRP model as a function of wind speed at 500 m, over land (top, z_0 = 0.03 m) and sea (bottom, Charnock coefficient = 0.0144) at four different stratifications: $T_s - T_a = -2^oC$ (dashed), 0^oC (solid), 0.1^oC (solid with circles) and 1^oC (solid with squares).

wind factor is constant. For instance, with typical open land $z_0 = 0.03$ m, the ratio is 0.62 for a 10-minute mean, or 0.69 for a 1-minute sustained wind. Increasing z_0 decreases the ratio, so over the sea, using the Charnock (or other) relation for z_0, the predicted ratio decreases as the wind speed increases. These respective variations are shown in Fig 1.15 (solid curves).

The effect of stability is that the surface-wind factor increases with increasing instability, with the wind speed dependence noted above superimposed. However, the stability effect is a quite nonlinear function, particularly at the transition from stable to unstable stratification. This is illustrated in Fig 1.15, which shows the variation of surface-wind factor with flight-level wind speed for four different air-surface temperature differences. It is clear that the impact of stratification is much greater for the unstable than the stable case, and in particular that a relatively substantial change is predicted when the air-sea temperature difference goes from zero to -0.1^{o}C, a difference which is at or below the limit of routinely available observations to detect. By comparison, the difference at tropical cyclone wind speeds between moderately stable and neutral stratifications is, for practical purposes, nonexistent.

1.3.5 Final remarks on theoretical and modelling studies

The simplest model of the atmospheric boundary layer which includes the effects of the earth's rotation is the Ekman spiral. In its classical form, as presented in many textbooks, the no-slip surface boundary condition leads to an over-estimation of the surface stress, with the consequence that the near-surface flow is too weak, and that the cross-isobar angle is too large. Reduction of the surface stress, either by the use of a semi-slip boundary condition, or a two layer model in which the turbulent diffusivity decreases toward the surface, corrects this error. In either case, the frictionally forced updraft is proportional to the curl of the surface stress. Further refinements to the theory can include the effects of baroclinicity, stability, and longitudinal roll vortices.

Similar boundary layer models for tropical cyclone-like vortices produce markedly different predictions to the straight, geostrophic flow case. Firstly, the updraft depends strongly on the surface boundary condition, with a semi-slip condition correctly organising the maximum vertical motion near the RMW, while the no-slip condition gives a quite uniform updraft across the eye. Secondly, the boundary-layer depth decreases towards the centre of the storm, although this effect could be counteracted by an increase in the turbulent diffusivity. Several studies showed weakly supergradient flow in the upper boundary layer, although it is difficult to attach much credence to the early numerical models due to the very large values of horizontal diffusion used. Weak outflow was often found above this maximum.

A slab model of the boundary layer of a translating cyclone found the strongest winds (which were supergradient) directly ahead of the storm, and somewhat inside of the gradient RMW. They were nearly colocated with the maximum frictionally forced updraft.

A one-dimensional profile model, which has been frequently used for estimating surface winds from aircraft measurements, was shown to produce lower values of the surface – aircraft wind speed ratio at high winds, and in stable conditions. The former variation arises in the model because of the increase in surface roughness of the ocean with wind speed.

1.4 Hypothesis and Scope of this Study

Consider the flow immediately above the boundary-layer in the core of a tropical cyclone. The thermal wind equation in cylindrical coordinates may be used to estimate the vertical shear. Here, values appropriate for a cyclone of moderate intensity are used; in particular a maximum wind of 40 m s^{-1} at a radius of 40 km, with a horizontal temperature difference of 2 K across the eye-wall, giving

$$\begin{aligned} \frac{\partial v}{\partial p} &= -\frac{R_d}{p}\left(\frac{2v}{r}+f\right)^{-1}\frac{\partial T}{\partial r} \\ &\approx -\frac{287}{9\times10^4}\left(\frac{80}{4\times10^4}+3\times10^{-5}\right)^{-1}\frac{2}{4\times10^4} \\ &\approx -8\times10^{-5}\ \text{m s}^{-1}\text{Pa}^{-1} \end{aligned} \qquad \textbf{(1.8)}$$

Thus, if gradient balance applies, there is a reduction in speed of less than 1 m s^{-1} in the 100 hPa immediately above the observed low-level maximum. Since the observed wind profiles frequently display much greater shear than this above the low-level maximum, it is plausible that the latter is supergradient.

The budget equation for absolute angular momentum M_a, defined by

$$M_a = rv + \frac{1}{2}fr^2 \qquad \textbf{(1.9)}$$

in cylindrical coordinates on an *f*-plane, is

$$\frac{DM_a}{Dt} = -\frac{\partial\varphi}{\partial\lambda} + K\left[\nabla^2 M_a + \frac{2}{r}\left(\frac{\partial u}{\partial\lambda} - \frac{\partial M_a}{\partial r}\right)\right] \qquad \textbf{(1.10)}$$

so M_a changes only through horizontal advection, azimuthal pressure gradients and

frictional torques. Here, u and v are the radial and azimuthal wind components respectively in the storm-centred cylindrical coordinate system (r, λ, z), φ is the geopotential, f is the Coriolis parameter, $\nabla^2 = \partial^2/\partial r^2 + 1/r\,\partial/\partial r + 1/r^2\,\partial^2/\partial\lambda^2 + \partial^2/\partial z^2$ is the Laplacian operator in cylindrical coordinates, K is the turbulent diffusivity for momentum (assumed constant), and $D/Dt = \partial/\partial t + u\partial/\partial r + v/r\,\partial/\partial\lambda + w\partial/\partial z$ is the rate of change following the parcel. The use of M_a is convenient for physical interpretation, since the Coriolis and centripetal terms in the azimuthal velocity equation in cylindrical coordinates are absorbed in the definition of M_a.

A steady-state, symmetric, stationary storm in a quiescent environment, thus requires a balance at all levels in the boundary-layer between radial advection, vertical advection, and turbulent diffusion of M_a. In an inertially neutral storm, the radial gradient of angular momentum (and hence its radial advection) is zero, while M_a increases outwards in an inertially stable storm. It is thus reasonable to expect that a sufficiently strong combination of inertial stability and inflow could produce a steady supergradient flow in such a storm.

However, the balance for the radial flow must also be considered. If the azimuthal component is supergradient, the imbalance between pressure, Coriolis and centripetal terms will tend to produce an outward acceleration of the radial wind at that level. Such a reduction or reversal of the inflow would upset the balance in the previous paragraph and lead to a weakening of the jet. Examining the balance equation for the radial flow in such a storm,

$$u\frac{\partial u}{\partial r} + w\frac{\partial u}{\partial z} - \left(f + \frac{v}{r}\right) v = -\frac{\partial \varphi}{\partial r} + K\left[\nabla^2 u - \frac{1}{r^2}\left(u + 2\frac{\partial v}{\partial \lambda}\right)\right] \quad \textbf{(1.11)}$$

it can be seen the possible candidates for maintenance of the inflow against the imbalance in the gradient wind part of the equation are inward and vertical advection, and turbulent diffusion. One possibility is that the inflow increases outwards from the storm centre, and is thus being maintained by self-advection. Another is that the inflow is greater below the level of the jet (above is implausible), and is being maintained at the level of the jet by upwards diffusion, and perhaps also upwards advection if the jet is located in an updraft. The contribution of turbulent horizontal diffusion is expected to be small.

Thus the central hypothesis for this study is as follows: *The low-level wind maxima observed in tropical cyclones are supergradient and steady-state, and are produced by inward advection of absolute angular momentum. The inflow at the height of the jet is maintained against gradient adjustment by some combination of advection and turbulent transport to be determined.*

While the preceding discussion has focussed on an axisymmetric storm, substituting typical values from the observational studies discussed above shows that the horizontal advection terms $u\partial u/\partial r \sim 10^2/(4\times10^4) = 2.5\times10^{-3}$ m^2 s^{-1} and $v/r\ \partial u/\partial\lambda \sim 40\times10/(4\times10^4\times\pi) = 3.2\times10^{-3}$ m^2 s^{-1} are of similar magnitude near the RMW. Thus the motion-induced asymmetry may well play an important role in the jet structure. Moreover, as the three-dimensional structure of this asymmetry is largely unknown, its study will form an important part of this thesis.

The focus will be on diagnosing the boundary-layer flow as the response to some known, gradient-level, forcing. Thus the influence that changes in the boundary-layer structure may have on the cyclone as a whole is ignored. While these clearly exist – for example, the pattern of boundary-layer convergence will affect the distribution of

convection and hence heating – the scope of this study is to explore just one side of what is undoubtedly a two-way interaction. There is also no attempt to resolve the effects of convection on the boundary layer, concentrating rather on larger scales. While studies (e.g. Powell 1990a, 1990b, Barnes and Powell 1995) have shown significant modulation of boundary-layer structure in the vicinity of rain bands, on scales comparable to the width of the band, this study focusses on building an understanding of the larger scale features of the tropical cyclone boundary layer.

Consistent with this focus on the boundary layer as a response to the "free atmosphere" flow represented by a parametric pressure field, and the neglect of convection, moisture is excluded from the models. Had it been included, its sole role (apart from that of passive tracer) would be a tiny contribution to the height variation of pressure, through the hydrostatic equation.

Finally, transient features that may arise due to instabilities in the prescribed vortex flow are also excluded. Again, while these may well be important in the real atmosphere, the concern here is with determining the steady, frictionally forced flow beneath an idealised, translating tropical cyclone.

These ideas are incorporated into a linear analytic model of the tropical cyclone boundary layer in Chapter 2, and into a numerical model in Chapter 3. In each, the boundary layer is regarded as the frictional response to a known, steady-state, tropical cyclone wind field in the "free atmosphere". Along with the properties of the jet, particular attention will be paid to the relationship between the near-surface wind and that aloft.

Summarising the above, this thesis examines the proposition that

The low-level wind maxima observed in tropical cyclones are supergradient and steady-state, and are produced by inward advection of absolute angular momentum. The inflow at the height of the jet is maintained against gradient adjustment by some combination of advection and turbulent transport to be determined.

- *The boundary-layer is regarded as the response to some known forcing in the free atmosphere, which will be prescribed.*
- *The effects of feedbacks from the boundary layer to the rest of the cyclone are assumed to be included in the prescribed free-atmosphere forcing, which will be chosen to be consistent with observations.*
- *Convective-scale processes, transients and instabilities are ignored.*
- *Moisture is ignored.*